TAMPEREEN TEKNILLINEN YLIOPISTO
TAMPERE UNIVERSITY OF TECHNOLOGY

NABID UZ ZAMAN BHUIYA FAIEM

AN ACTIVE ELECTRODE BASED ECG MEASUREMENT SYSTEM FOR MINIMALLY SPACED PRECORDIAL BIPOLAR LEAD

Master of Science Thesis

Examiners: Prof. Jari Hyttinen and
Prof. Matti Mäntysalo
Examiner and topic approved Faculty Council of the Faculty of Computing and Electrical Engineering on 02 May 2018

ABSTRACT

Nabid Uz Zaman Bhuiya Faiem: An Active Electrode based ECG Measurement System from Minimally Spaced Precordial Bipolar Lead
Tampere University of technology
Master of Science Thesis, 63 pages, 01 Appendix pages
May 2018
Master's Degree Programme in Electrical Engineering
Major: Electronics
Examiners: Prof. Jari Hyttinen, Prof. Matti Mäntysalo

Keywords: Single Supply Active Electrode, Inter-Electrode-Distance, DC coupling ECG, Potentially Driven Right Leg ECG.

Electronics miniaturization leads the development of small wearable Electrocardiography (ECG) devices. These devices are getting special attention due to current trends in Human-Computer-Interaction applications and remote patient monitoring. Therefore, user comfort is an essential requirement for these kind of devices where the number of electrodes and the distance between the electrodes is kept short. This short inter-electrode-distance (IED) degrades the signal quality which leads to poor signal-to-noise ratio (SNR). In this thesis, a novel measurement system was developed to record ECG from bipolar chest lead with short IED.

The measurement system was developed with single supply, low noise active electrode (AE) and ADS1299 Evaluation board (EVM) to evaluate the performance of active electrode with ADS1299 ECG analogue-front-end (AFE). The low noise, high input impedance, and precision components were given priority during the design of the AE. The performance of the developed system was carried out by testing common mode rejection ratio (CMRR), SNR and frequency response. The system was used to record ECG signal with commercial product BN-RSPEC module with different IED in diagonal orientation near the heart's main axis.

The single supply AE+ADS1299 system demonstrated excellent noise performance over the specified bandwidth of 262 Hz. The system also demonstrated high CMRR at 50 Hz. The most noteworthy accomplishment of this thesis was that the developed system is capable of recording P wave from the midsternum with a short IED of 0.3 cm. Although the measurements were performed on a single subject, this system outperforms the BN-RSPEC module from BIOPAC Inc. in recording from the close spaced electrodes.

PREFACE

I would like to give special thanks to my thesis examiners Prof. Jari Hyttinen and Prof. Matti Mäntysalo for providing me the great support throughout the thesis. I would also like to special thanks to Jouko Heikkinen for teaching me the PCB fabrication and Milla Jauhiainen for providing the assistance during the measurements in HEAT lab.

I would like to thanks my friends and family for providing me the support throughout the life.

Finally, I would like to give credits my billions of neurons for generating electrical signals during the thesis.

Tampere, 28.6.2018

Nabid Uz Zaman Bhuiya Faiem

CONTENTS

LIST OF FIGURES

LIST OF SYMBOLS AND ABBREVIATIONS

ECG	Electrocardiography
IED	Inter-electrode-distance
CVD	Cardiovascular diseases
WHO	World Health Organization
ΔΣ ADC	Delta-sigma analog-to-digital converter
AFE	Analogue-front-end
EVM	Evaluation board
SA	Sinoatrial
AV	Atrioventricular
SNR	Signal-to-noise ratio
AAMI	Advancement of Medical Instrumentation
ANSI	American National Standards Institute
IEC	International Electrotechnical Commission
AHA	American Heart Association
CMRR	Common mode rejection ratio
RLD	Right-leg-Drive
AE	Active electrode
DR	Decimation ratio
ENOB	Effective Number of Bits
EMG	Electromyography
PDA	Personal Digital Assistant
S/H	Sample and hold
ZNP	ZigBee Network Processor
GUI	Graphical User Interface
FDA	Food and Drug Administration
CAM	Carnation Ambulatory Monitor
HRV	Heart Rate Variability
AVDD	Analog voltage supply
PGA	Programmable gain amplifier
AAF	Antialiasing filter
FSR	Full scale range
IRN	Input referred noise
SPS	Sampling per second
V_{cm}	Common mode voltage
V_{ref}	Reference voltage

1. INTRODUCTION

The aim of this thesis is to develop a novel cardiac monitoring system to record electrocardiography (ECG) in normal living conditions. The miniature electronics lead to the development of small, wearable healthcare products that are yet more powerful and less susceptible to noise. These small devices also demand to reduce the inter-electrode-distance (IED) and open the possibility to record new kind of electrophysiological signals. Furthermore, these small devices are offering more user comfort so that it can be worn for a long time without leaving any trace on the body. For this reason, these devices are suitable for biofeedback applications in the Human-Computer-Interface system as well as for the individual who has cardiovascular diseases (CVD).

CVD that indicate the disorder of the heart and blood vessels are the most dominant reason for death globally [1]. According to the fact sheet of World Health Origination (WHO), approximately 17.7 million people died in 2015 because of CVD. These diseases are flagged as number one reason for death around the globe. Most of these deaths can be prevented if early precaution could be taken. [2] Thus the status of the heart needs to be monitored 24/7 for those who have a chance to develop these diseases.

An ECG device can give the status of the heart instantly as heart generates electrical activity. It becomes an essential part of the diagnostic tool for those having cardiac problems. The first ECG device which was invented in 1901 by Dr. Willem Einthoven, a Dutch physiologist, weighed about 270kg [3]. Physicist Norman Jefferis Holter was the first person who developed the idea of a portable ECG device or ambulatory ECG, and thus the portable ECG recording device is referred as Holter monitor. The clinical use of this Holter monitors began since early 60's. [4] With the development of miniaturized electronics, these devices are becoming smaller; thus it can be worn for longer periods of time, recording typically for 24-48 hours. These devices use lead cables to record ECG, and thus cable movement is a critical issue along with motion artifacts for these kind of devices.

Recently a tremendous improvement has been achieved in the field of wearable ECG device. Several companies are manufacturing chest straps and wrist watches for long time heart rate monitoring. As the size of these devices are becoming smaller, it is essential to reduce the spacing between the electrodes. The proximity of electrodes reduces the signal quality as well as the signal morphology which is a crucial factor for small size wearable devices. In addition to this, the measurement location and electrode orientation also play a critical factor for small wearable devices [5]. Thus to develop a wearable system, these impacts must be taken into consideration.

The primary goal of this thesis was to develop the wearable ECG measurement system that can measure ECG from closely spaced electrodes from the thorax. Besides, the effect of measurement location for short IED was also evaluated with a standard measurement system.

Low noise and high precision electronic components and delta-sigma analog-to-digital converter (ΔΣ ADC) architecture were given priority in the design for better noise performance. The system was developed with active electrodes (AE) and a medical analogue-front-end (AFE) which is suitable for low noise, high precision bio-potential measurement. The AE was introduced in the system to overcome the problem of skin preparation, to reduce the power line interference and the motion artifact. The single supply AE was designed as the ADS1299 AFE drives the subject with a DC potential. The ADS1299 evaluation board (EVM) from Texas Instruments was chosen which incorporates the medical AFE, ADS1299. After evaluating the electrical characteristics of the developed system, the next part was to evaluate the performance of the developed system as a wearable system. The evaluation was performed by recording with disposable electrodes simultaneously with the BN-RSPEC module from the BIOPAC systems for long and short IED in different locations on the chest.

2. THEORETICAL BACKGROUND

This chapter provides the background information of the origin of electrical activity of heart, ECG recording techniques as well as the requirements for developing the small wearable device. This chapter also provides a review of other smaller ECG devices and their performance in clinical experiments.

2.1 Biology behind Electrocardiogram

The heart locates inside of the mediastinum within the thoracic cavity and weight about 250-300 g [1, 6] . The heart is separated into four chambers: two atria and two ventricles. The blood enters from the atria and forces back to the circulation system by the ventricles. The interatrial septum divides the two atria while the interventricular septum separates the ventricles. The blood flow direction is controlled by four different valves that are located between the atria and the ventricles and between the ventricles and the arteries. The heart wall is mainly composed of cardiac muscle tissue known as the myocardium that provides the mechanical force to pump the blood back to the circulation system. The cardiac muscle fibers are coupled by intercalated disks that have low electrical resistance gap junctions. [1, 7]

Heart muscles work rhythmically to pump blood to the circulation system. A rapid change in the membrane potential of the cardiac muscle cell or myocyte is marked as the initial phase of the cardiac action potential that recognized as depolarization. This rapid rise of voltage depends on the combination of ion concentration. Depolarization spreads to the neighboring cells as myocytes can conduct action potential to its adjacent cells. The membrane potential gradually returns to its resting state known as repolarization. [7]

The sinoatrial (SA) node consists of a special type of cells known as pacemaker cells that spontaneously fire electrical impulses. The generation rate of this action potentials is typically 60-100 per minute which determines the heart rate in resting condition. Then the action potential travels to the atrioventricular (AV) node and the left atrium. The left atrium is depolarized through a particular type of conductive cells known as Bachmann's bundle. The action potential travels to the AV node with 50 milliseconds delay moreover AV node takes another 100 milliseconds to pass the action potential through it. This delay provides enough time to fill up the ventricles with blood before contraction. Then the action potential travels towards the bundle of His and then to the left and right bundle branches. Both the left and the right branches run down towards the direction of the apex of the heart to connect with the Purkinje fibers. Finally, the Purkinje fibers spread the action potentials extremely fast throughout the ventricular muscles from the apex of the heart toward the base of the heart and the atrioventricular septum. Depolarization of these

muscles activates the adjacent contractile cells to push the blood to the circulation system. Finally, depolarization is followed by repolarization then the cycle starts again. [1] The resultant of these different action potentials are superimposed in the ECG signal which is shown in Figure 1.

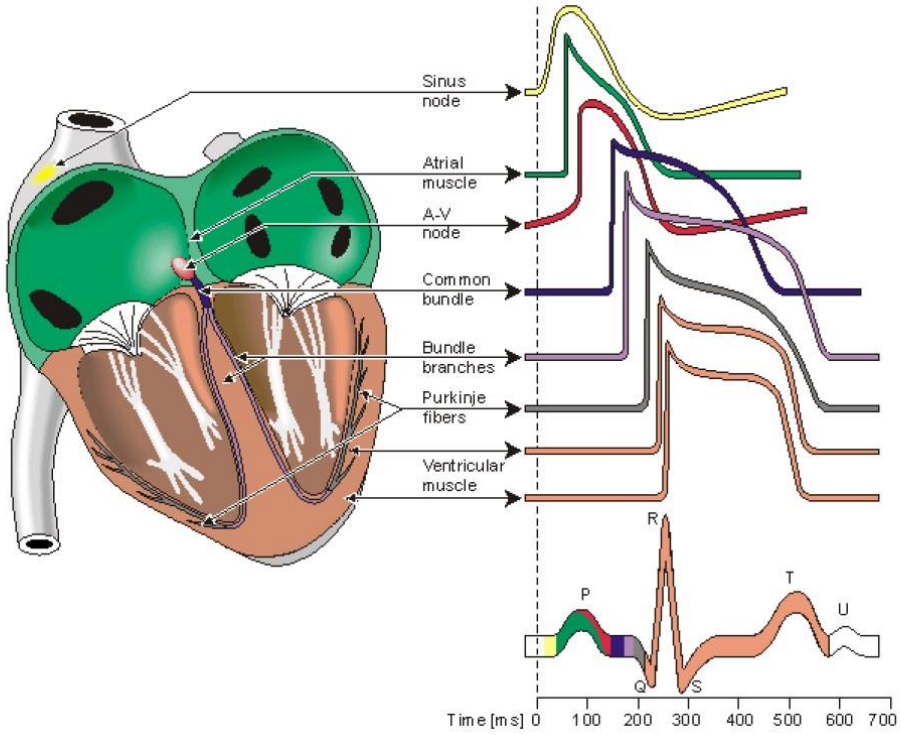

Figure 1. *The conduction system of the heart. The action potentials from different types of cells contribute the formation of ECG [6].*

2.2 Electrocardiography

ECG is a standard tool for measuring the electrical activity of the heart. The summation of these action potentials that originated from the different segments of the heart, can be measured from the surface of the body by placing two electrodes. The pair of electrodes is known as the lead, and the potential difference between these electrodes is known as the lead voltage. A typical ECG waveform is similar to Figure 1 contains three primary features: the P wave, the QRS complex and the T wave. The depolarization of both atria reflects in the P wave. Due to the small amplitude and the short duration of the P wave, it is hard to distinguish from noise. The magnitude of P wave is minimal because of the small muscles area in the atria in contrast ventricles have large muscle area thus the depolarization of ventricles (QRS complex) show strong potential. The duration of QRS complex is typically 70-110 ms and composed of three waves Q, R and S wave. T wave represents the repolarization of the ventricles. [7] Multiple leads are used to evaluate the

heart from the different angle. The 12-lead is the standard system used in the clinical diagnostic.

2.2.1 Standard 12 Lead ECG

The conventional 12 lead ECG consists of six chest leads and six limb leads. The six chest leads are V1-V6, and these are measured with Wilson's central terminal (WCT) and termed as unipolar. In contrast, six limb leads are divided into three bipolar limb lead (I, II and III) and three augmented lead (aVR, aVL, aVF). Augmented leads are the same electrodes that are used for the lead I, II and III but these leads are unipolar and obtained from each limb electrode referenced against the average of other two limb electrodes. Six limb leads provide the vertical view of the heart in contrast six chest lead offer the horizontal view. Although 12 lead system provides the valuable information about the heart, the electronic miniaturization offers a new opportunity for new kind of ECG device for cardiac monitoring more efficiently. [6]

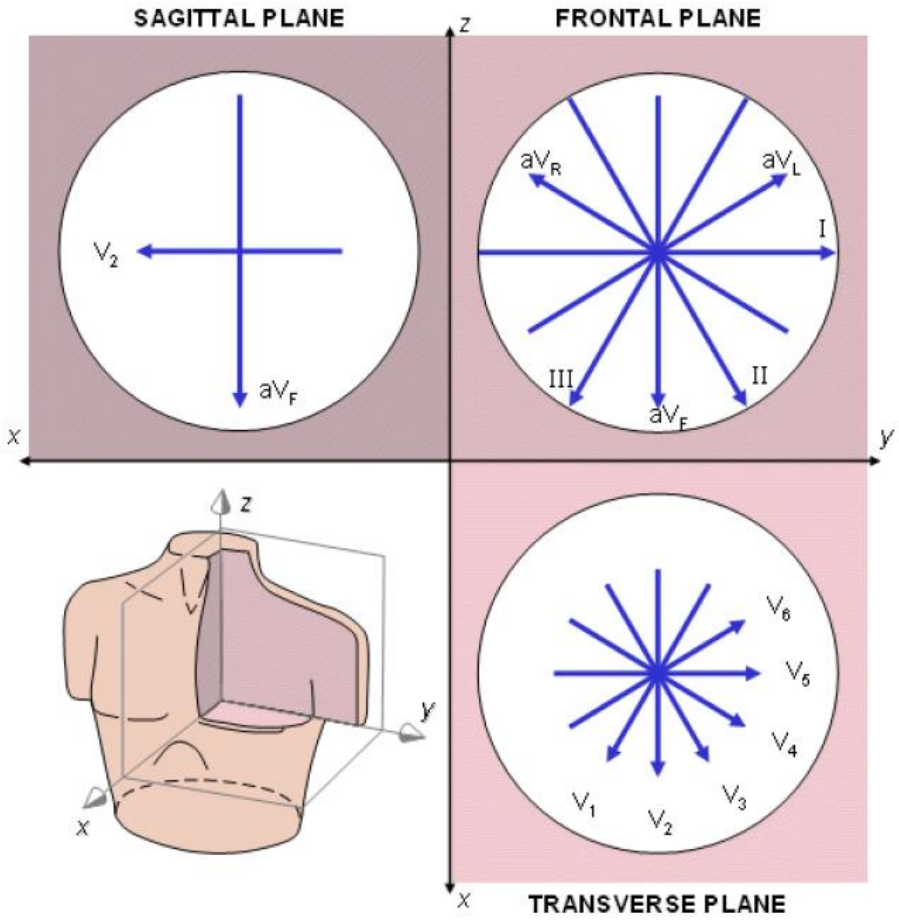

Figure 2. *Lead vector representation of 12-lead ECG [6].*

2.2.2 Skin-Electrode Contact Interface

It is necessary to know the anatomy and physiological properties of the skin to understand the interaction between skin and electrode. The human skin has three primary layers. The outermost layer is epidermis, and the inner layers are the dermis and the subcutaneous layer. The stratum corneum of the epidermis which contains dead cells and dry cells makes contact with the electrode. The impedance of this layer is different from the other living tissue. Neuman and Webster developed the skin-electrode interface model which is visualized in Figure 3. [8]

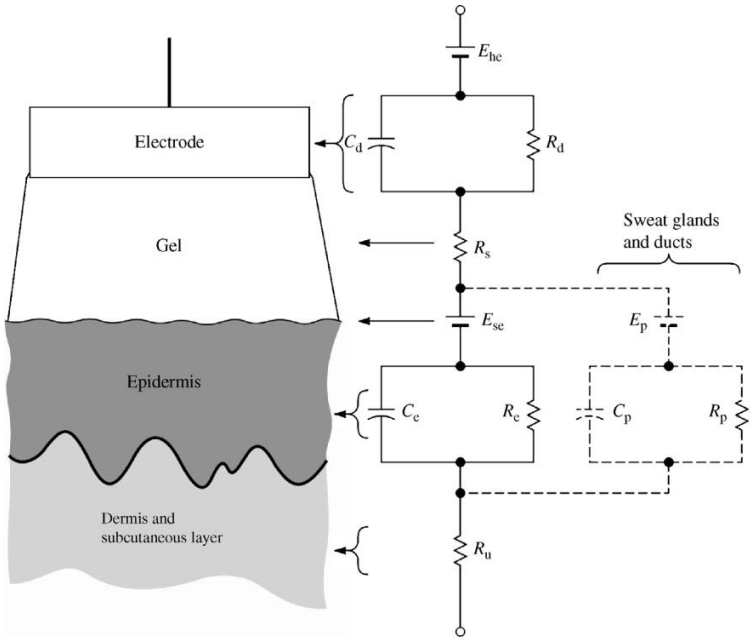

Figure 3. *Equivalent Electrical Model Skin-Electrode Interface [8].*

The model in Figure 3 represents the equivalent electrical model of the skin-electrode interface. This model considers all skin layers as those are on the pathway of the signal. The dermis and the subcutaneous layer act as a pure resistor, while the epidermis layer is modelled as electrical impedance and potential difference E_{se} due to the different ionic concentration in stratum corneum as this layer is semi-permeable to ions. The conductive sweat creates a potential difference between the sweat duct and extra-cellular membrane, and the electrical model of sweat duct is represented as R_p and C_p. Highly conductive gel of electrode shows only the resistive property R_s and the electrode impedance is represented as R_d and C_d. Ionic current converts into electric current between the electrode and the electrolytic interface. This interaction happens due to the electrochemical reaction that exchange ion electron at the interface. [8]

2.3 Wearable ECG

Although the standard 12-lead ECG is widely used as the clinical diagnostic tool, the portable and wearable ECG devices are becoming more popular as the device size is minimal and user-friendly. The standard 12-lead system provides information about the heart activity from different angles whereas small wearable ECG device with short IED can include information about the particular part of the heart [5].

Miniaturized electronics make it possible to build small ECG device with the short IED. Moreover, it is possible to detect local myocardial activity rather than the total activity of the heart. If the specific part of the heart is targeted to identify the local myocardial activity, then it is now possible to detect with an acceptable signal-to-noise ratio (SNR). The potential field of the heart dipole is much stronger for bipolar leads that are placed near to the heart. The potential field becomes weaker with the cube of the distance. [9] Bipolar lead can be placed in such a way that it can detect the particular property of the heart [5]. So called aimed lead was developed by Jari Hyttinen in 1994 that can detect the local electrical activities of specific part of the heart such as local myocardial activation [10].

The critical requirement for small wearable ECG device is to record the low amplitude ECG signal as the electrode proximity is small. Moreover, as the signal strength varies with the location, the electrodes need to be placed diagonally in the particular position to record the signal with an acceptable SNR [5].

2.3.1 Design Requirement for Small Wearable ECG Device

Several guidelines have been introduced to standardize the cardiac monitor or ambulatory ECG devices by different organizations such as EC 13 standard by the Association for the Advancement of Medical Instrumentation (AAMI)/American National Standards Institute (ANSI), International standard 60601-2-47 by International Electrotechnical Commission (IEC). [11] The ECG device is becoming smaller day by day due to the advancement of miniature electronics thus it is necessary to update guidelines more frequent.

The American Heart Association (AHA) Electrocardiography and Arrhythmias Committee, the Council on Clinical Cardiology, the American College of Cardiology Foundation and the Heart Rhythm Society released an updated technical guideline for diagnostic ECG recording in 2007 which was endorsed by the International Society for Computerized Electrocardiology [12]. The previous technical guideline from the ad hoc writing group of the Committee on Electrocardiography and Cardiac Electrophysiology of the Council on Clinical Cardiology and the AHA was published in 1990[13]. These guidelines are emphasized on the digital based ECG in clinician environment. [12, 13] The details about the ECG amplifier characterization was provided in earlier recommendation that was published in 1967 [14].

AHA recommended in recent guidelines to set the lower cutoff frequency at least 0.67 Hz. The minimum requirement for upper cutoff frequency was recommended to 150 Hz as most of the diagnostic information of the QRS complex is below 100 Hz. The minimum sampling rate for digitalizing the analog input signal is 500 Hz to reduce the amplitude error to ~1%. [12] The minimum ADC quantization noise of 10 μV_{pp} was recommended for bandwidth of 150 Hz [12, 13]. The minimum requirements for ECG recording from the guidelines mentioned above are provided in Table 1.

Table 1. *Minimum Requirement from AHA Technical Guideline for ECG. [12, 13]*

Parameter	Recommended Value
Lower Cutoff Frequency	0.67 Hz
Upper Cutoff Frequency	150 Hz
ADC Resolution	8 bit/sample
ADC Quantization Noise	10 µV
ADC Sampling Rate	500 Hz

ADC plays a critical role in the noise level of ECG AFE designing. The quantization noise in 24 bit ADC is much lower compared to the standard introduced in the guidelines mentioned above. The quantization noise less than 50 nV is already available in 24 bit ADC by several commercial companies. The resolution of ADC also determines the number of components in the ECG input signal path. There are two approaches in designing of the ECG AFE which is based on the resolution of the ADC.

A high gain amplifier is essential for low-resolution ADC based design. In this approach, high pass filter is critical to remove the DC component otherwise it will saturate the amplifier. Moreover, low pass filter is the essential part of the signal path otherwise high-frequency interference can couple into the signal. The designer needs to take special consideration for choosing low noise amplifier and high precision components to reduce the overall noise level and CMRR. [15]

In contrast, the high resolution 24 bit ADC provides an opportunity to reduce the hardware complexity as DC coupled ECG can be recorded by this type of ADC [11]. Moreover, the 24 bit $\Delta\Sigma$ ADC works on oversampling technique where the lower frequencies

noise is suppressed. The oversampling allows reshaping the noise until the band of interest and the function of digital decimator filter is to reduce the higher frequency and quantization noise. Furthermore, the decimator filter relaxes the complex antialiasing filter by a single 1st order RC filter. [16] In this approach, a low gain amplifier is sufficient as the resolution of the ADC is higher and because of the low gain amplifier, DC component cannot saturate the amplifier thus DC component can be stored and processed in the digital domain. [15]

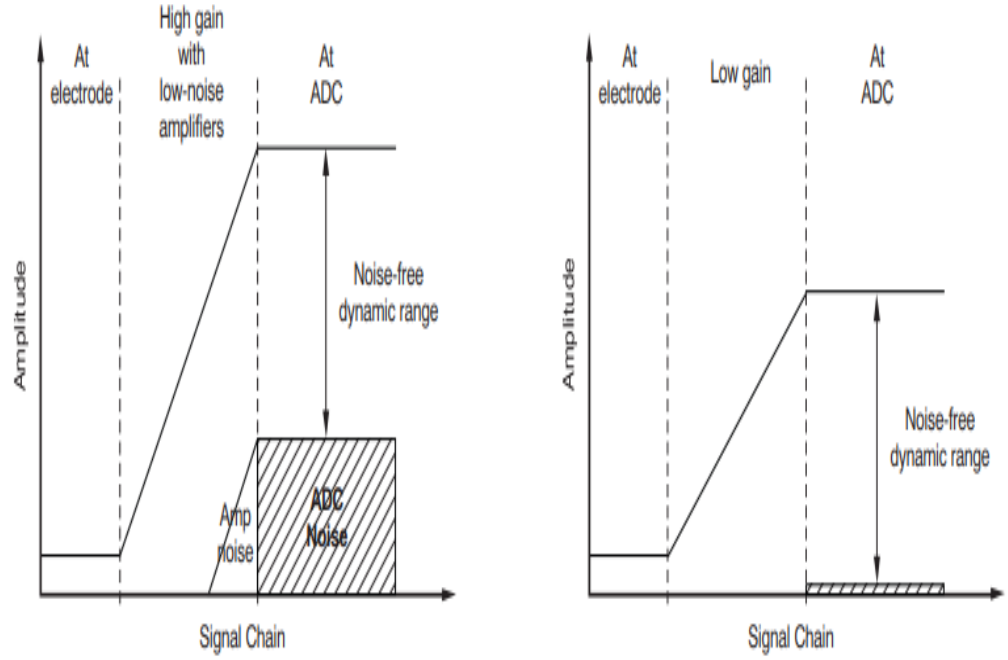

Figure 4. *Different Design approach based on the resolution of ADC [15].*

The design complexity increases in the low resolution ADC system and noise is amplified with high factor by the amplifier. In contrast, the right side of Figure 4 represents the high resolution ADC approach where the noise floor is kept minimal. [15]

2.3.2 Electrode Location

The electrode placement for short IED bipolar ECG device is a critical factor as the signal strength varies in individual level. Puurtinen et al. recommended in 2009 that the location of the electrodes depends on the application of ECG device [17]. Diagonally placed electrodes around the V1 and V2 precordial electrodes provide a better signal strength to record the P wave. The optimal location for detecting the QRS complex is diagonally placed electrodes around V2, V3 and V4 electrodes as this positions lies within the heart axis. Figure 5 shows the best location for detecting ECG signal from chest for small ECG

device. Although the heart axis varies on the individual's anatomical structure thus to predict the signal level in individual level is difficult. [17] However, their indications are very useful to develop a new wearable ECG device. This thesis is based on their lead orientation to evaluate the P wave and QRS complex.

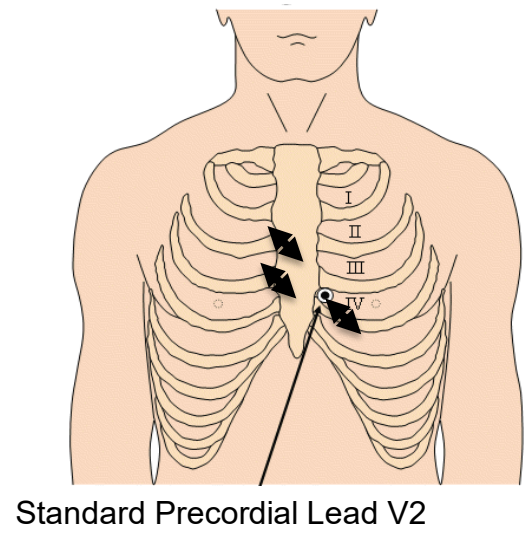

Figure 5. *Best location for small precordial ECG measurement [17].The image was modified from [6]*

2.3.3 Factors Affecting the ECG Recording

As the distance between the electrodes is very short thus the signal can be effected easily by noise. There are several factors that affect the signal quality. The noise sources can be classified into several sources: environmental interference, electronics noise, biological artifacts, motion artifact and movement artifact. Biological artifacts originated within the subject's body whereas the environmental interference, thermal noise, and electronics noises arise outside the body. The following sections describe the sources of the noise in details.

Environmental Interference (50 Hz Noise)

Different electromagnetic sources such as power lines, cellular phone and radio transmitter surround the earth atmosphere. Even in a home environment, the human body can peak several millivolts with respect to ground which is several times larger than ECG signal. [18] The interaction between the power line and the human body is modelled as a capacitor C_2 in Figure 6. The effect of this ac power line is visible as 50/60 Hz sinusoidal

signal in ECG measurement similar to Figure 7. The difference in the skin-electrode impedance causes further interference in ECG signal as cables also coupled with the AC main and modelled as capacitor C_{CB}. Figure 6 represents the coupling model between AC main to the ECG system. [8]

The effect from 50/60 Hz main signal can be minimized by using battery-powered ECG system. In this situation, the impact of C_B capacitor is reduced as both grounds are different. This effect can be further improved by using a high common mode rejection ratio (CMMR) differential amplifier. Moreover, both input of the amplifier receives the same common mode voltage at its input. With the advancement of electronics, it is now possible to use an amplifier with high CMMR typically -120 dB at 50/60 Hz. Furthermore, the Right-leg-Drive (RLD) or Bias Drive technique can be used to reduce the common mode noise. In this technique, the common mode voltage is sampled from the inputs of the amplifier, further amplified and fed back through Bias electrode. [8]

Additionally, high CMRR differential amplifier with an AE can be used to reduce the power line interference [19]. An op amp in buffer configuration can be used to transform the impedance can reduce the power line interference.

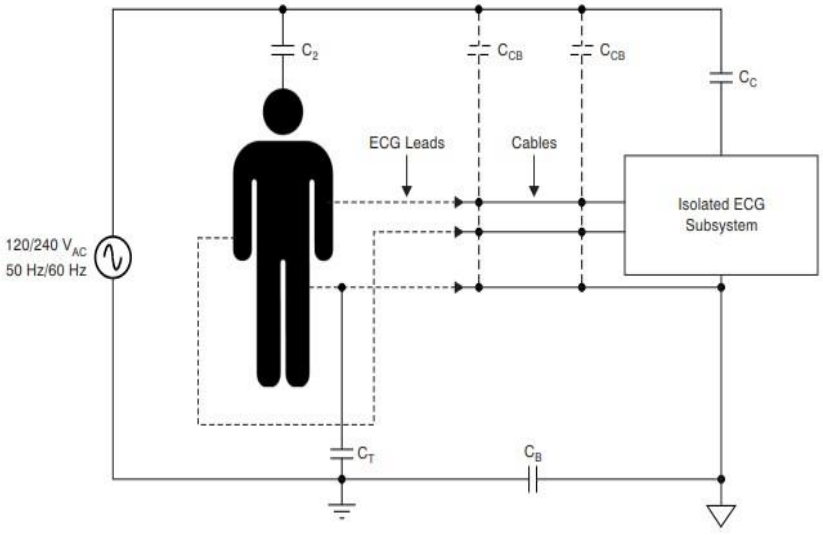

Figure 6. *Capacitive coupling with AC main [20].*

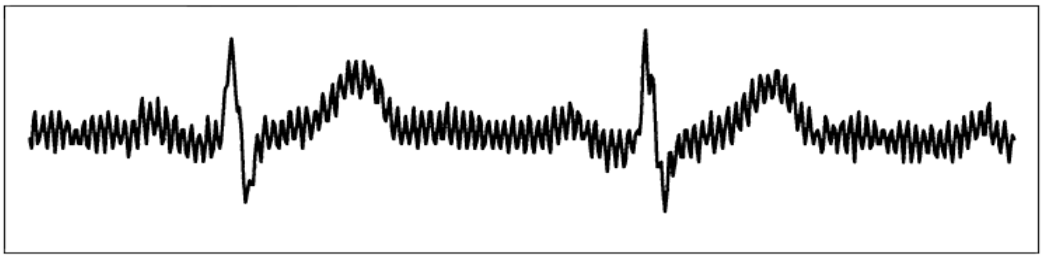

Figure 7. *50/60 Hz main interference [18].*

Thermal Noise

The movement of electrons depends on the temperature. The random motion of electrons at the temperature above zero Kelvin creates a current for a short period and cancel out in momentarily by each other. However, a specific imbalance is present. This random thermal agitation can be identified as high-frequency noise which is known as Johnson noise. [21]

Thermal noise is calculated from Nyquist equation

$$e^2 = 4kTR\Delta f \quad (1)$$

where

e = Voltage due to thermal noise
k = k is Boltzmann's constant (1.38–23 joule/Kelvins)
T = Temperature in Kelvin
Δf = frequency difference in Hz
R = R is resistance in Ω

Thermal noise cannot be removed, and it always remains even without the presence of external current. But from the equitation (1), it is possible to reduce noise by reducing the frequency bandwidth and by lowering the resistance.

Another source of thermal noise is the skin-electrode contact interface. The skin electrode interface are modeled 51 kΩ resistor shunt with 47 nF capacitor for gel electrode which is specified by AAMI. At room temperature, the thermal introduced at the interface is equal to 591 nV_{pp}. [22]

Electronic Noise

There are two types of noises: white and pink noises that are associated with an Op Amp. Pink noise or the flicker noise has a dominant effect on the lower frequencies while white noise is the primary source in the higher frequencies. The corner frequency separates these two regions. The noise of Op Amp is modelled as a voltage source and a current source. These sources are the mixture of both white and pink noise. Voltage noise and current noise is calculated from the following equation, [23]

$$E_n = e_{nw}\sqrt{f_{ce} * ln\left(\frac{f_H}{f_L}\right) + f_H - f_L} \tag{2}$$

$$I_n = i_{nw}\sqrt{f_{ci} * ln\left(\frac{f_H}{f_L}\right) + f_H - f_L} \tag{3}$$

where e_{nw} & i_{nw} are the white noise, and f_{ci} and f_{ci} are corner frequencies. The frequency bandwidth of the system is $\triangle f = f_H - f_L$.

High precision amplifiers offer very low voltage noise as well as current noise which are typically below 10 μV voltage noise and current noise in fA range [23]. Special consideration must be taken during the design of the small wearable device as the input noise might become a dominant factor if right Op Amp is not considered.

As the signal strength is weak in the small wearable device thus noise level of ADC must be minimal. The input referred noise (IRN) of ΔΣ ADC depends on the sampling frequency (f_S) of delta-sigma modulator and output data rate of decimator filter (f_D). The relationship between f_S and f_D determines the decimation ratio (DR) as can be seen from equation 4. The delta-sigma modulator in the ADC drives the low frequency noise to

higher frequencies and the digital decimation filter removes the high frequency noise as well the quantization noise introduced by the delta-sigma modulator. The Effective Number of Bits (ENOB) depends on the DR. High ENOB can be achieved by keeping DR higher. In Figure 8, the ENOB is higher for lower output data rate, but it decreases with the increased data rate. [16]

$$DR = \frac{f_S}{f_D} \qquad (4)$$

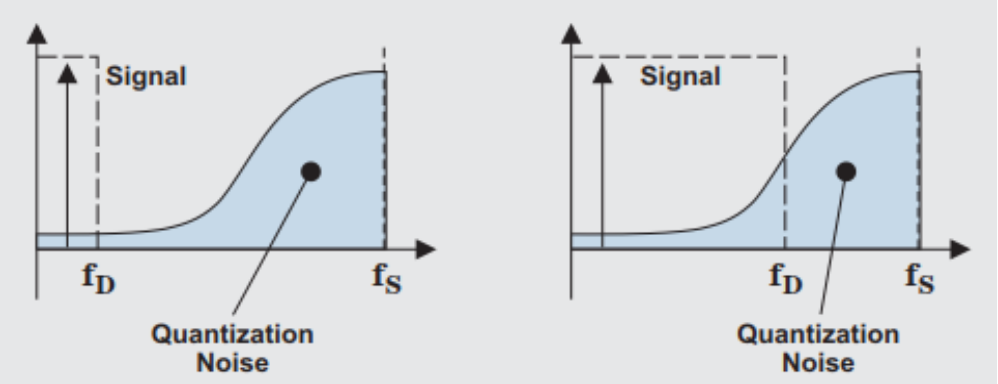

Figure 8. *Quantization Noise shaping of ΔΣ ADC [16].*

The higher clock frequency can improve the ENOB in the second scenario of the Figure 8 as the modular frequency depends on the clock rate [16].

Biological Artifacts

Biological artefacts originated as electrical activities within the human body from other sources than the source of interest. Other sources such as muscle activities, respirational activities create electrical signals such as Electromyography (EMG) and the respiratory signal. Digital filters can be introduced to remove out of interest biological signals.

Motion Artifact

Motion artifact is another major artefact source in the wearable ECG device that occurs in the ECG bandwidth which arises due to the deformation of upper layer of epidermis and the disturbance of half-cell potentials at the electrode-electrolyte interface [8, 18]. The deformation of skin causes unstable contact between skin and electrodes, changes in half cell potential of electrolyte, changes in skin impedance, and cable movement. [24]

As mentioned in section 2.2.2, the stratum corneum is composed of dehydrated and dead cells thus this layer is 30 mV negative compared to the highly conductive living tissue layer of the dermis. The deformation of the skin decreases this potential to about 25 mV and the rest 5 mV appeared as motion artifact. [25] The deformation also causes changes in the skin impedance. The frequency dependent skin impedance has higher magnitude from 10 kΩ to 1 MΩ in lower frequency at 1 Hz. The skin impedance gradually decreases in higher frequencies. At frequency higher than 1 kHz, the impedance reduced to around 10 kΩ. [26] The stratum corneum of the epidermis layer is the main contributor for this high impedance at low frequency of 10 Hz [27].

Gel electrode that contains conductive gel as mentioned in 2.2.2 provides a stable physical and electrical connection against the horizontal and vertical forces at the skin-electrode interface although this layer becomes dry over time. On the other hand dry electrodes or un-gelled electrodes lack this layer show a large contact resistance. Dry electrode depends on the skin moisture. Although sweat is highly conductive but it does not provide uniform contact as gel electrode does thus a small deformation in skin causes a large change in the electrical properties of skin-electrode interface. [24, 28]

Most common way to reduce the effect of the stratum corneum by removing this layer by rubbing the skin with sandpaper. This reduces the overall impedance of the skin as the high impedance source is removed. This procedure is not suitable for wearable application also it can causes of infection as the outer layer of the skin removed. [24]

The effect of epidermis also can be minimized by introducing a special type electrode. Cömert et al. developed a special type of dry textile electrode in 2013 with soft padding support that stabilize the skin around the electrode to minimize the motion artifact [29]. The soft padding works as a buffer when lateral force is applied to electrodes either from the epidermis or clothing. The comparatively larger area of padding stabilize the surrounding area of epidermis around the electrode. [30]

The deformation of skin causes two different impedance signal at the input of differential amplifier which reduce the CMRR of the system. This impedance imbalance can be prevented by introducing AE. AE transform the high impedance source signal in to low impedance signal [31, 32]. AE can be designed with high input impedance amplifier in voltage follower configuration at the sensor side to reduce impedance imbalance [31].

The effect of cable movement can be cancelled by introducing cable less design such as patch devices.

2.4 Review of Small Portable ECG Devices

This section provides a review for small ECG devices, introduced by several researchers and commercial company that use bipolar lead. The information was obtained from the reference and citation from the paper of Puurtinen et al.[17]. The commercial products were found from the internet search by using a keyword small portable or ambulatory ECG device. The small ECG devices typically contain electrodes and the electronics in a single unit without a lead cable thus it refers as wireless ECG by some researchers. These devices are attached to the body by some adhesive materials, and typically wet gel electrodes are used. With the advancement of ADC technology, these small devices are getting particular attention. This section will provide a short introduction about the small ECG systems, and later the technical features and measurement systems will be discussed in the following sections.

2.4.1 Technical part of the Systems

A small size ECG device with shortest IED was introduced by Russel et al. where they used a prototype that developed by Philips Medical Systems, Seattle, WA. The miniature ECG prototype had the minimum distance of 2.48 cm between a bipolar lead. The prototype, introduced by Russel et al. in 2007, contained three bipolar leads. The spacing between electrodes was 2.48 cm and the total system was less than 10 cm in its largest dimension which is shown in Figure 9. The device had the capability of recording ECG for15 hours and can be attached to the skin by adhesive material. The sampling rate of the prototype was 300 Hz, and the analog signal was converted to the digital environment by 12 bit resolution ADC. [33]

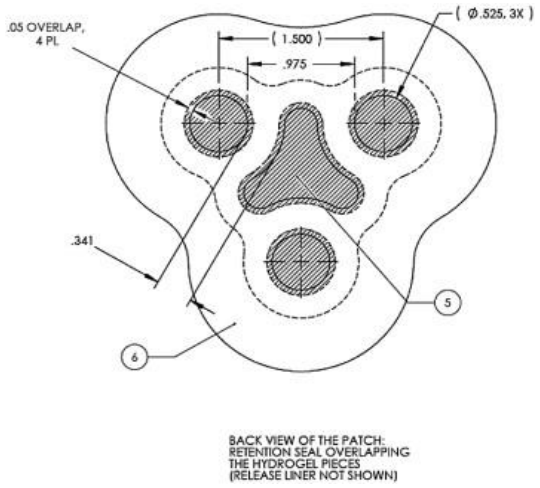

Figure 9. *The short spaced electrode patch for the prototype developed by Philips Medical Systems [33].*

Another remarkable miniature ECG device was developed in 2004 by Fensli et al. where they used 3 cm spacing between electrodes of a bipolar lead. They also introduced the concept of wireless ECG system for continuous monitoring. The wireless ECG monitoring system introduced by Fensli et al. had three parts. The first part of the system had an ECG sensor circuit, modulated RF transmitter, nRF401 and two 3V Li/MnO_2 battery. The second part of the system had an nRF401 based receiver, ATmega8L-8AI microprocessor which includes 8-bit ADC. The receiver was connected to a PDA (Personal Digital Assistant) by a RS232 cable. The differential input range of the ECG sensor was ± 5 mV with a gain of 250 and having the bandwidth of 0.5-150 Hz. The sensor used only a bipolar lead without ground electrode to measure ECG for 5 hours. [34]

Munshi et al. introduced a small ECG device in 2008 by integrating an ECG chip developed by them. The wet gel sensors in the bipolar lead configuration was incorporated in their device with distance only 5 cm. The integrated solution provided by Munshi et al. for wearable ECG device was implemented in small Printed Circuit Board (PCB) (55 mm x 23 mm) that contained electrodes slot for a bipolar lead, ECG chip, RF Transceiver CC2430, micro SD card slot and rechargeable 3.7 V Lithium Polymer battery. The developed ECG chip had a low noise amplifier, a sample and hold (S/H) circuit, and a 12 Bit SAR ADC. The IRN of the chip was 2.1 μVRMS for the 3-dB bandwidth of 0.052 -200 Hz. The CMRR of the system is greater than 67 dB. The sampling frequency of the system is 1000 Hz. The chip had a mid-band gain of 45.5 dB. Their developed did not include the RLD or Ground electrode in the measurement. [35]

Wang et al. presented a new three lead system for wearable ECG device in 2013 for long-term home care monitoring. Their lead system consists of three bipolar leads that were placed in such way that the distance between two horizontal electrodes was 5 cm and the vertical distance between these electrodes and a ground electrode was 6 cm [36, 37]. The wearable device developed by Wang et al. consists of three parts which are the ECG AFE, the End-Device and the Coordinator. The End-Device and the Coordinator were implemented by TI CC2530 ZigBee Network Processor (ZNP) Mini Development Kit. The designed the ECG AFE with an instrumentation amplifier (INA333from Texas Instruments) with a gain of 200. The introduced a high pass filter to remove DC offset and a second-order Sallen-Key low pass filter with OPA333 from Texas Instruments. The bandwidth of their system was 0.04-40 Hz and having CMRR of 100dB. The microcontroller MSP430F2274 in the End- Device had 10 bit SAR ADC which had the sampling frequency of 200 Hz. The sampled signal was transmitted to the Controller to process the data in MATLAB GUI (Graphical User Interface). [36]

Trobec et al. developed a commercial ECG sensor system, Savvy, which is capable of recording of reliable ECG from small spaced bipolar lead [38]. Their early prototype also used 5 cm spacing between the bipolar lead in 2010 [9, 39]. A commercially available wireless body sensor, Savvy ECG was developed by Trobec et al. from their seven years of experience in developing ECG sensor. The first prototype had only an ECG sensor

later they introduced temperature sensor and accelerometer. In the early prototype, electrodes were connected directly to the sensor board whereas in the final prototype they included a single cable to increase the flexibility of the system. The multifunctional prototype consists of ECG front end microcontroller, BLE, and lithium coin cell battery. The resolution ADC of the microcontroller is 10 bit and sample the input signal by 200 Hz. The -3 dB bandwidth of the system was 0.15 – 250 Hz. The prototype includes only bipolar lead without having RLD/Ground electrode. [9, 39]

Another small spaced wearable system was designed by Uddin Akib in 2014 in University of Toronto. The developed ECG system is capable of measuring ECG from the chest with 10 cm spaced electrodes. Uddin Akib designed a wearable sensor with the dedicated biopotential AFE ADS1293, accelerometer LIS3DH and BLE microcontroller CC2541. The ADS1293 AFE from Texas Instruments had 3 channel, but only one channel was used in this design in the bipolar configuration. The sampling rate of the system was 260 Hz, and the resolution of the ΔΣ ADC which is built inside of the AFE is 24 bits/sample. The complete sensor was embedded in a patch module that included the slot for wet electrodes that were separated by 10 cm. The sensor also utilized the RLD electrode to minimize the ac main noise. [37]

Among commercially available products ZIO® XT Patch (iRhythm Technologies, Inc., San Francisco, CA) [40]. ZIO® XT is a non-invasive wearable patch that intended for recording ECG from the chest for 14 days. This sensor has one bipolar lead that collects data with 200 Hz sampling rate, and the resolution of this device is 10 bits. The electrode separation is less than 12 cm that connected to the body with adhesive materials. This device is intended for single use only, and the device needs to be sent to the Zio Service after recording is complete where FDA (Food and Drug Administration) approved machine learning algorithm is applied to analyze the patient data. [40]

Carnation Ambulatory Monitor™ (Bardy Diagnostics, Inc., Seattle, WA) [41] showed a potential performance as small ECG device. There is no technical information available for the Carnation Ambulatory Monitor (CAM) from the developer company. But as the spacing between the bipolar electrodes is 11.5 cm, and the device is intended to place on the sternum to record the atrial activity especially thus it is included.

The comparison between the device specifications that presented above and the standards are demonstrated in Table 2. Most of the device follow the standards specified by AHA [12, 42] except the epatch® and ECG AFE which are intended to measure in low frequency of the ECG. Moreover, the sampling rate requirement also violated by some of these devices.

Figure 10. *ZIO®XT patch (Left)[40] , Carnation Ambulatory Monitor (Right) [41].*

Table 2. *Comparison between the Standard and Device Specification*

Device	IED (cm)	Lower Cutoff Frequency (Hz)	Upper Cutoff Frequency (Hz)	ADC Resolution (bit)	ADC Sampling Rate (Hz)	ADC Quantization Noise (μV)
AHA Specification[12, 42]	-	0.67 Hz	150	8	300	10
Philips Medical Systems [33]	2.48	-	-	12	300	2.54
ECG Sensor [34]	3	0.5	150	8	500	19.54
Prototype ECG AFE [36]	5	0.04	40	10	200	-
ECG Plaster Device [35]	5	0.052	200	12	1000	2.1
Wearable ECG [37]	10	-	-	24	260	-
Prototype Device [39]	5	0.15	250	10	200	-
ZIO® XT[40]	12	0.15	34	10	200	-
ePatch® [43]	11	0.67	40	12	512	146

2.4.2 Measurement System

This section describes the clinical experiments for devices mentioned above. Most wearable ECG devices were evaluated with standard equipment mostly knowns as Holter monitor. Holter monitor is used for recording ECG for a shorter period typically 24-48 hours. Several monitors have developed since it is widely in the clinical environment. [5] The detailed descriptions of the experiments are discussed in this section.

The small ECG prototype introduced by Russel et al. was evaluated with a standard Holter monitor (Philips Zymed DigiTrak Plus 24-hour recorder) in the clinical environment in 2010. In this experiment, 143 patients having cardiac arrhythmias were involved. The sampling rate was adjusted to 200 Hz to evaluate with the Holter monitor. The electrode patch was placed at the sternum whereas the electrodes of the monitor were configured as EASI lead configuration similar to Figure 11 (left). Both devices recorded ECG concurrently for 15 hours [44]. Another experiment was conducted earlier in 2007 with the same prototype. Total 90 patients were included in the experiment who had cardiac symptoms. This experiment was performed in the Department of Emergency Medicine, General Hospital of Vienna. The prototype was placed at four different locations in the chest (below left clavicle, midsternal, below left breast and left antrior axillary line in the 5th intercostal space) similar to Figure 11(right). Similarly, the recording was done simultaneously with the Philips Zymed DigiTrak monitor. In both cases, the skin was prepared before the prototype device was attached to the skin. The electrode configuration for both experiments is presented in the Figure 11. [45]

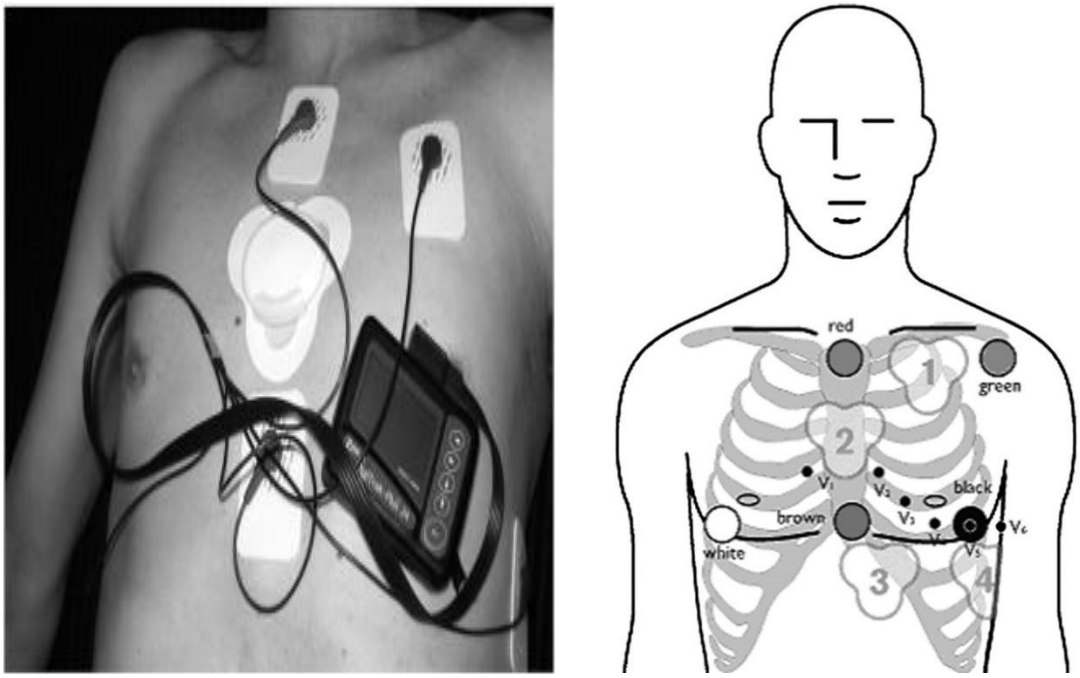

Figure 11. *Electrodes placement to evaluate the performance of the prototype. (Left) The electrode patch was placed at sternum to record strong cardiac arrhythmia. (Right) The four electrode patches were connected in four different locations. In Both cases the Holter monitor is attached to the thorax in EASI configuration (E = brown, A = black, S = red and I = white). [44, 45]*

Fensli et al. developed their ECG sensor for long time monitoring as an alternative to a Holter monitor and a cardiac event recorder. Their sensor was connected to the body by a bipolar lead separated by 3 cm from each other and conductive gels were applied to the skin to reduce the skin contact impedance. The sensor was attached to the subject's chest by adhesive tape as the sensor as the sensor size is minimal. [34]

Wang et al. developed a lead system as mentioned in section 2.4 to evaluate the performance of their device. Their new bipolar three leads system was placed close to each other in small place. They followed the Mason-Likar limb lead system as the standard system for their measurement where they labelled the electrodes that put in the chest as LA, RA, LL and RL. From these electrodes, they reconstructed the standard lead as Lead I = RA-LA, Lead II = LL-RA and Lead III = LL-LA. Later, they reduced the distance between the electrodes thus the horizontal distance between the electrode LA, and RA was 5 cm, and the distance between LL-LA and RA-LL became 6 cm. The RLD electrode was placed in between the RA and LA electrodes. [36]

The recent prototype developed by Trobec et al. was measured with closely separated electrodes in bipolar configuration on a single person. The electrodes were placed around the sternum with IED of 5 cm. The sensor used adhesive wet gel electrodes to connect the sensor to the body. [39]

Uddin Akib developed a small wearable device is capable of measuring ECG signal from the chest. The patch module where the electrodes were configured as standard Lead I configuration with the 10 cm spacing between the electrodes. The device was evaluated at the location suggested by Lim et al. [46] and Puurtinen et al. [17] to detect the R-Peak for HRV (Heart Rate Variability) analysis. [37]

The performance of ambulatory Zio-XT patch system was studied by Barrett et al. for 146 patients. The single bipolar device was placed at left chest near the sternum of the patients as Figure 12 and instructed to wear for as long as possible up to 14 days. The patients were also fitted with a Holter monitor to record ECG for 24 hours. [47]

CAM patch system was evaluated in a clinical experiment by Smith et al. with a standard 3-lead Holter system (NorthEast Monitoring, DR 180 Series) for over 24 hours in the clinical environment. These devices were used simultaneously on 50 patients who have cardiac rhythm problems. The bipolar CAM system was placed on the sternum and the Holter system used 3 channel (7 electrodes) was placed as [48] as shown in Figure 13.

Figure 12. *The placement and orientation of Zio Patch Module [47].*

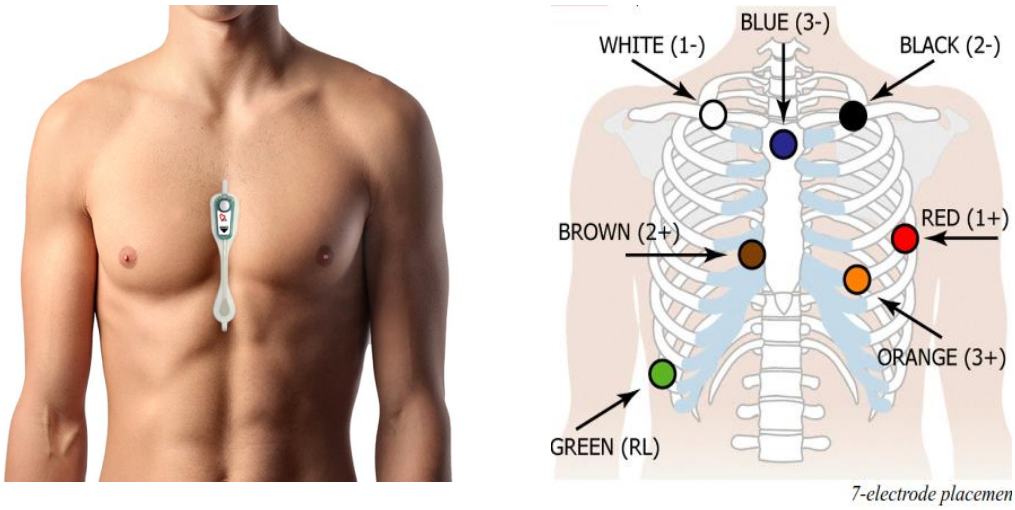

Figure 13. *The Bipolar lead of CAM system placed on the sternum (Left) [41]. The electrode placement and orientation for 3 channel system (3 channel and Green electrode is dedicated for RL/Ground) of Digital Recorder [49].*

2.4.3 Results from the Review

This section provides the results obtained from the experiments mentioned above. Only the result of the clinical research will be discussed as they carry significant patient participation.

The experiment was conducted to evaluate the prototype of Philips Medical Systems shows a significant result. In the early research in 2007, they found good quality ventricular activity in all locations, but specific atrial activity was observed in mid sternum location even with the small electrode distance. They found the presence of P wave, PR interval and rhythm with 94-98 % accuracy in this location whereas the only 58-80% P wave was present in Philips Zymed DigiTrak monitor recording. [45] In the later experiment which was conducted in 2010, they found the prototype was capable of identifying ventricular arrhythmias with reasonable accuracy as well as the correlation coefficient between the monitor and the prototype was quite high. They also indicated that although the correlation coefficient was high but not perfect which might be due to the short lead field and unconventional location and orientation of the device. [44]

The experiment led by Barrett et al. found that the Holter monitor detected more arrhythmia events than the Zio patch in first 24 hours of recording although the total number of arrhythmia events detected by Zio patch was more than the Holter device. The overall detection of arrhythmia events was 96 in Zio patch whereas 61 events were recorded in the monitor. [47]

The study conducted by Smith et al. concludes that CAM system is capable of reliable P wave from the sternum area compared to the Holter monitor used in the experiment. As the CAM system is placed on the sternum which is near to the right atrium thus this system is identified as the potential candidate for diagnostic use. They also indicated that the comparatively good SNR of CAM system along with its placements in sternum enables for recording high-quality atrial activity. [48]

The results from these experiments also indicate that the small ECG device is capable of capturing the atrial activity with reasonable accuracy when the device is placed near to the atria (precordial V2 lead). The location of the Zio Patch reduced the capability of recording the presence of P wave with accuracy alternatively CAM patch system outperformed the Holter monitor in capturing P wave. The results from these experiments also agree with the optimal locations found by Puurtinen et al.[17]. Moreover, the sensors used in these experiments were placed in the same unit with the electronics thus cable movement artifact and inference induced by AC main to the cable was reduced. The device mentioned in section 2.4 has significantly small IED although with this small IED they found an acceptable result. The short IED reduce the SNR. Moreover, the shorter lead and unconventional lead orientation reduce the signal quality for P wave drastically. Thus it is necessary to consider the placement of the device very accurately. The prototype

from the Philips Medical Systems showed a significant result even with the shortest IED by capturing the acceptable signal with 12 bit ADC where the 1 LSB corresponded to 2.5 µV for 200 Sample per second (SPS) [33]. The advancement in the ADC technology makes it possible to record the smaller signal with high quality than this prototype. The 24 bit ADC has high resolution, and the 1 LSB is much lower than the prototype. This advantage can incorporate to wearable ECG devices to record high-quality ECG signal in short distance.

3. MATERIALS AND METHODS

The primary objective of the thesis was to develop a small wearable device for the chest to record high-quality ECG signal. The findings from sections 2.4.3 were considered for designing the system.

The signal strength of the short chest lead is very weak, thus low noise components and high-resolution ADC were considered during the design stage. The block diagram of the system is presented in Figure 14. The system was designed with two active electrodes and an ADS1299 EVM from the Texas Instruments.

The small ECG signal from the short bipolar chest lead fed to the battery powered active electrodes, and from there it proceed to the low noise ADS1299 AFE of EVM. The sampling rate of the system was set to 1000 Hz to achieve the bandwidth of 262 Hz, and the gain was adjusted to 24. The resolution of the ADS1299 AFE was 24 bits/sample. More specifics of the system is provided in next sections.

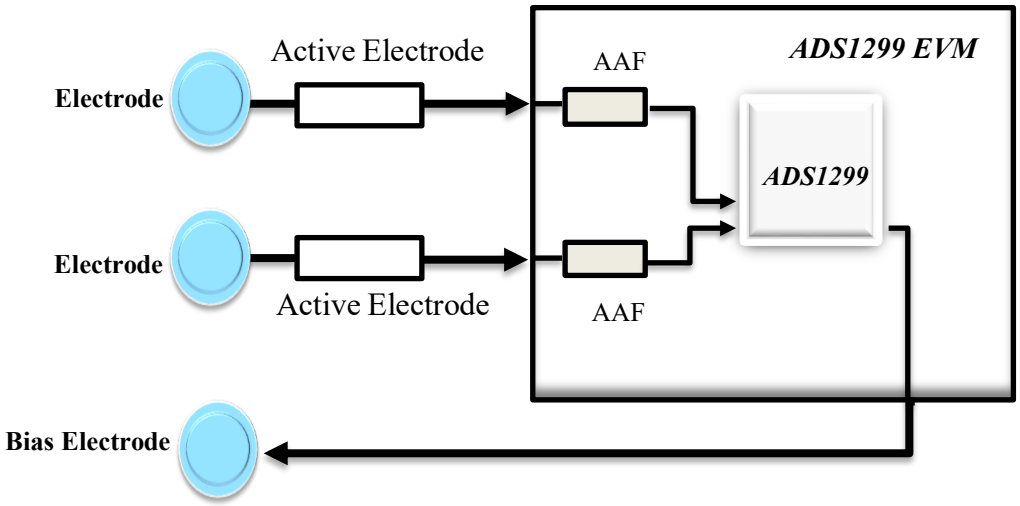

Figure 14. *Block Diagram of the short bipolar lead ECG measurement System.*

3.1 Electrodes

The first component in the signal chain is the bio-potential electrodes. An electrode is a transducer that converts ionic current to electric current. Bio-potential electrodes for wearable application can be divided into three groups that are gelled electrodes, dry electrodes and non-contact electrodes. Among these types of electrodes, gelled electrodes provide both electrically and physically stable connection because these electrodes are covered with a conductive gel medium known as the electrolyte. In contrast dry electrodes such as textile electrodes lack this conductive medium. Non-contact electrodes measures bio-potential capacitively without directly connected to the skin. [24] Although the textile electrodes are getting special attention for wearable applications but in this thesis only gelled electrodes were used to evaluate the performance of the AE and the measurement system for short chest bipolar leads.

Non-polarized Ag/AgCl is the most common type of commercially available electrode which has low half-cell potential. The benefit of this non-polarized electrode is that current can pass freely in the interface. In addition to this, this type of electrode provides very low noise which is suitable for the small wearable solution. [8]

Although Ag/AgCl is a standard tool for ECG diagnosis but sometimes due to the difference in half-cell potential of two electrodes the skin introduce excess DC voltage in the measurement. Moreover, input bias current of the amplifier can polarize the electrode when there is poor contact between the electrode and skin. [8] Furthermore, the conductive gel dries out after several hours causing impedance imbalance of electrodes that reduce the signal quality [31]. Thus to minimize the impedance imbalance of the electrodes active electrode was introduced in the design.

Two different types of standard Ag/AgCl electrodes from Ambu® were used in this thesis. The dimensions of these electrodes are tiny which is suitable for the small wearable application. These disposable sensors provide a strong adhesion as well which is essential for stable physical connection. The dimension of adhesive area and sensing area of these two types of electrodes are presented in Table 3 [50, 51]. The Blue Sensor P from Figure 15 (a) has larger adhesive area compared to the Blue sensor N from Figure 15 (b) but the sensing area is smaller in Blue Sensor P.

Table 3. *Key Characteristics of Blue Sensor P and Blue Sensor N. [50, 51]*

Electrode Dimensions	Blue Sensor P	Blue Sensor N
Electrode Size (in mm)	34 (Diameter)	44.8 x 22 (L x W)
Electrode-Skin Contact Size (in mm)	34 (Diameter)	30 x 20 (L x W)
Sensor Area (in mm^2)	10	15
Adhesive area (in mm^2)	754	556

Figure 15. *Ambu® BlueSensor P (Left) [50],Ambu® BlueSensor N (Right) [51].*

3.2 Active Electrode

Motion artifact and dry out of conductive layer of gel electrodes introduce impedance mismatch [31, 52]. To improve the mismatch of impedance can be reduced by introducing AE in the system [31]. A simple AE can be built by using an op amp in voltage follower manner at the input stage of the measurement system [32, 53]. The primary function of the AE is to transform the high impedance bio-potential signal to low impedance. The advantage of using AE is that it reduces the power line interference and motion artifact does not need any skin preparation which is an attractive feature for the wearable solution. [31, 32]

In this thesis, the AE consist only a buffer amplifier to convert high impedance signal source to low impedance signal. Thus the AE is able to balance skin-electrode contact impedance which is a crucial factor for low noise recording. The AE used a single power supply as the bias amplifier of ADS1299 AFE provides a fixed DC potential of 2.5 V (AVDD/2). This potential drives the subject's input common mode voltage within the rails of AE. Thus this configuration allows to design AE with only a single power supply and dc coupled input signal. During the design of AE, following characteristics was given priority a) High Input Impedance, b) Low input bias current, c) Low voltage noise, d) Low current noise.

Table 4. *Important Electrical characteristics of OPA2140. [54]*

Parameters	Value Typical	Max	Unit
Input Impedance			
Differential	10^{13} || 10		Ω || pF
Common Mode	10^{13} || 7		Ω || pF
Input Bias current	±0.5	±10	pA
Input voltage noise			
f = 0.1 Hz to 10 Hz	250		nV_{pp}
f = 0.1 Hz to 10 Hz	42		nV_{RMS}
Input voltage noise density			
f = 10 Hz	8		nV/√Hz
f = 100 Hz	5.8		nV/√Hz
Input current noise density			
f = 1 kHz	0.8		fA/√Hz

Table 4 shows the critical parameters of the OPA2140 that are suitable for designing AE. The low noise parameters make an ideal candidate for the small wearable device. Moreover, the input impedance is much higher 10 T Ω so that the recorded signal will not be attenuated.

3.2.1 Simulation

The AE presented in Figure 16 was designed with only one protection resistor R_P and one OPA2140 JFET Op Amp. The purpose of the protection resistor was to provide a minimum level of protection during the fault condition. The supply voltage of AE is 6.6 V thus in worst case 6.6 V/ 100 kΩ = 66 µA will pass through the body. This current is higher than the standard safety limit of 50 µA introduced by AAMI [8].

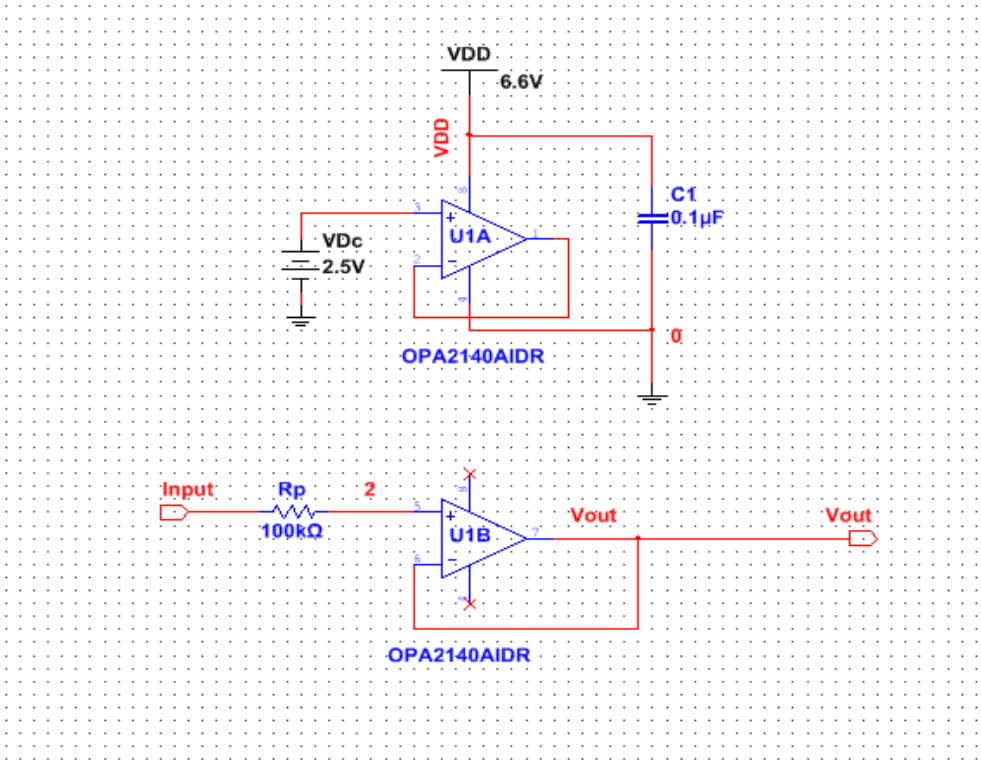

Figure 16. *Schematic diagram of single supply AE circuit. The amplifier was designed as voltage follower configuration to convert the high impedance source signal to low impedance signal.*

As the bias of the ADS1299 AFE can potentially drive the subject thus the AE was designed with the single supply. The supply circuit was designed with only two CRC2032 coin cell batteries and a voltage divider circuit to provide the common voltage to unused op-amp. The un-used amplifier was terminated with 2.5 V that was similar to the common

voltage supplied by the bias circuit of the ADS1299 AFE. The termination helps to avoid extra noise caused by unused op amp the in the system. The schematic was drawn in the circuit design software NI Multisim 14.1 from National Instruments. The simulated frequency response of this AE is presented in Figure 17 where the -3 dB bandwidth of this AE is 230 kHz. In the simulation, AC analysis magnitude was set to 1 V_{p-p} with 2.5 V DC offset.

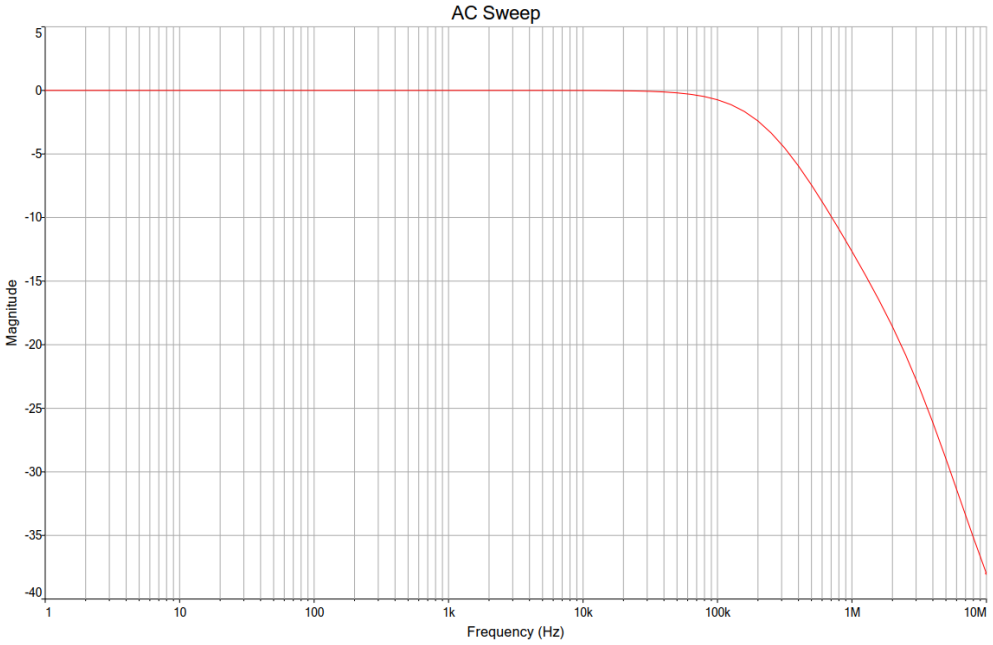

Figure 17. *The frequency response from the simulation of AE circuit for 1 V_{p-p} with 2.5 V_{DC} offset. The -3 dB Bandwidth of this system was found 230 kHz.*

3.3 ADS1299 ECG Front End Evaluation Board

The advancements in high precision, miniature electronics and ADC technologies lead the advancement of medical AFE. Texas Instruments developed several medical AFE since the last decade for recording low amplitude bio-signals. The integrated solution in ADS129x by incorporating low noise Programmable Gain Amplifier (PGA), ΔΣ ADC, BIAS (RLD circuit) in a single chip. They also provide evaluation board where they incorporate ADS129x chip with different filters. This evaluation offers the readymade solution to test the AFE performance in different environment and design. In this thesis, ADS1299 evaluation board is used with the developed AE to measure low amplitude ECG signal from the chest. The main features of this evaluation are discussed in next sections.

3.3.1 Anti-Aliasing Filter

The purpose of antialiasing filter (AAF) to attenuate the out band signal thus noise from the high frequency does not reduce the SNR [55]. The decimation filter of ΔΣ ADC relaxes the sharper frequency response of AAF. Therefore a simple 1st order RC low pass filter can be used to remove high frequency content. The evaluation board uses a 1st order RC filter before the PGA input with low tolerance components [56]. The –3 dB corner frequency of the AAF can be calculated by using equation 5. [55]

$$f_{cm} = \frac{1}{4\pi R C_{CM}} \tag{5}$$

The corner frequency f_{cm} of the AAF used in the EVM is 6.8 kHz.

3.3.2 Programmable Gain Amplifier

The AAF is connected to the input of the PGA of ADS1299 AFE. The PGA is a low noise fully differential input and output amplifier having the gain of 1,2,4,6,8,12 and 24. The fully differential input signals depend on the reference voltage (V_{ref}) of the system and gain configuration. The input signals swing around the common mode voltage (V_{cm}) in fully differential configuration as Figure 18. The full scale range of the input signal is $\frac{2V_{REF}}{Gain}$. [57]

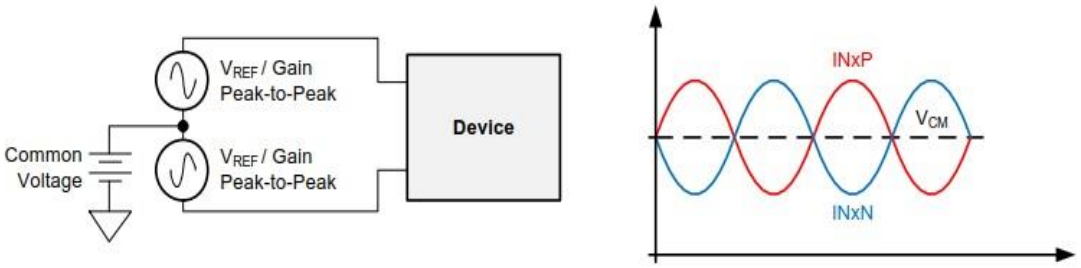

Figure 18. *Fully differential configuration of PGA input signal swing around common voltage and depends on the gain settings [56].*

The V_{cm} and full scale range (FSR) of input signal is calculated by following equation, [56]

$$ADVV - 0.2V - \frac{(Gain*V_{MAX})}{2} > V_{CM} > AVSS + 0.2V + \frac{(Gain*V_{MAX})}{2} \quad (6)$$

$$V_{MAX} = \frac{2*V_{REF}}{Gain} \quad (7)$$

For gain 24, V_{CM} ranges from 0.3 V to 4.7 V and the maximum differential input range is ± 187.5 or 375 mV.

3.3.3 24-Bit Delta Sigma ADC

The 24-bit ΔΣ ADC is the core of ADS1299 AFE as it allows the DC coupled low amplitude signal measurement with high resolution. The ΔΣ ADC consist of a second order ΔΣ modulator and a digital decimation filter.

The ΔΣ modulator has a 1-bit converter that converts the analog input signal into modulated pulse wave with a higher sampling rate f_{mod} than the Nyquist frequency, and this technique is known as oversampling. The quantization noise produced by the 1-bit converter is shaped into higher frequencies by using the combination of oversampling technique and integrators in the system. The ADS1299 uses second order to shape the noise even further into high frequencies.

A digital decimation filter can attenuate the high-frequency noise and the high data rate introduced by the ΔΣ modulator. The filter consists of a third order sinc filter which is responsible for mitigating the high-frequency noise and convert the 1-bit data into a 24-bit data. In addition to this, the modulator data rate f_{mod} is decimated into lower output data rate f_d without losing any information. The frequency domain transfer function of this sinc filter is established by equation 8,

$$H(f) = \left| \frac{\sin\left(\frac{DR*\pi*f}{f_{mod}}\right)}{DR*\sin\left(\frac{\pi*f}{f_{mod}}\right)} \right|^3 \quad (8)$$

where DR = Decimation Ratio from equation 4. The DR depends on the filters output data rate and modulator sampling rate. The frequency response of the equation 9 depends

on the DR. The DR becomes higher for the narrower frequency range, and DR becomes lower for higher bandwidth. Thus for higher bandwidth, ENOB becomes lower as it includes high frequency noise. [57]

The second order ΔΣ modulator digitizes the analog signal from the PGA at the rate of $f_{mod} = f_{CLK}/2$ where the f_{CLK} is the clock frequency. The f_{CLK} = 2.048 MHz for the EVM thus f_{mod} would be 1.024 MHz after that the DR can be configured from the EVM software (CONFIG1 Register) and the corresponding f_{mod} will be applied to the digital filter. The decimation filter has infinite notches at multiple of f_d and the passband of the filter repeats after every f_{mod}.

The AAF has a corner frequency f_{cm} of 6.8 kHz which less than $f_{mod}/10 = 10\ kHz$. Thus there is enough attenuation before the passband of the digital filter.

3.3.4 BIAS and Common Mode Rejection

The bias amplifier of ADS1299 provides a bias voltage to the subject during single supply configuration to maintain the common mode voltage within the rails of the ADS1299. This feature allows measuring the DC coupled signal. Besides, the bias amplifier provides a negative common mode noise feedback to the subject to reduce the AC main interface. [54] This configuration provides a better solution to remove common mode noise as it samples the output signal of the PGA, amplified it and fed back to the subject via bias drive electrode.

A common voltage of 2.5 V was applied from the ADS1299 AFE to the subject to reduce the common mode noise as well as to provide the bias voltage.

3.4 Measurement Module Testing

Following electrical tests were conducted to verify the performance and functionality of the system.

3.4.1 Noise

As mentioned in the section 2.3.3, there are three primary sources of noise in the electronics system. Each noise was analyzed differently. The thermal noise from the protection resistors and anti-aliasing filter was calculated from the equation 1, and the voltage and current noise from the AE were calculated from equation 2 and 3. The thermal noise of ADS1299 (at 1000 SPS and Gain = 24) is taken from the datasheet [57].

The IRN of the system was tested as Figure 19 by shorting the inputs of AE+ and AE- to a DC potential of 2.5 V from the battery circuit, and the output of AE+ and AE- was connected to the channel 2 of ADS1299. All other channels of ADS1299 were shorted together and connected to the same voltage of 2.5 V from the battery circuit as well so that it would not contribute interference to the system. The noise test was done for 10 seconds, and the output signal was recorded in the ADS1299 EVM software and later analyzed in the MATLAB. This setup is adapted to measure the internal noise that is generated by the measurement system.

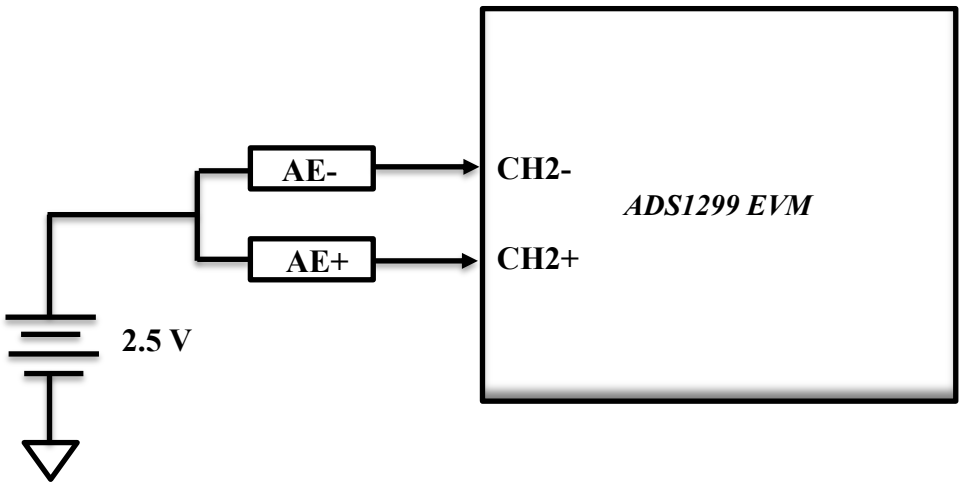

Figure 19. *Test Setup for measuring the input referred noise of the system. The input of both AE were shorted together and connected to a DC voltage of 2.5 V. The outputs of AE were connected to the positive and negative terminal of the channel 2 of ADS1299 EVM.*

3.4.2 Common Mode Rejection Test

The common mode rejection test was employed by shorting the two inputs of AE+ and AE- and connected to a V_{cm} of 1.6 V_{P-P} with 2 V Dc offset from the function generator as demonstrated in Figure 20. The frequency range for this measurement was chosen from 1 Hz to 500 Hz. All other channels of the ADS1299 EVM were shorted together as well and connected to 2 V from the battery. In this setup, the differential gain of ADS1299 was adjusted to 24, and the output data rate was also adjusted to 1000 SPS. The common mode gain, A_{CM} was calculated from the equation 9 which is the ratio of output and input signal amplitude. After that, the CMMR was derived from the equation 10. The output signal was recorded in the ADS1299 EVM software.

$$A_{CM} = \frac{V_{OUT}}{V_{CM}} \tag{9}$$

$$CMRR = 20 * \log_{10}\left(\frac{A_D}{A_{CM}}\right) \tag{10}$$

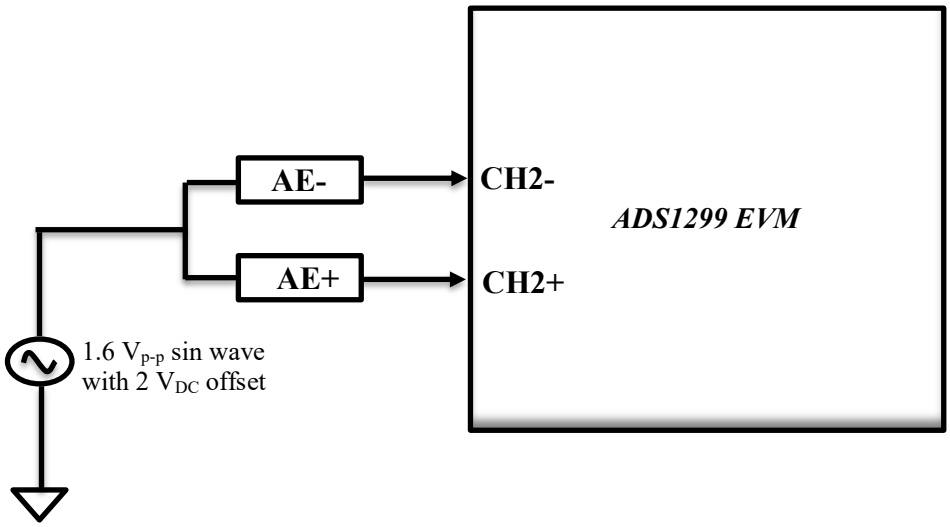

Figure 20. *Test setup for measuring the common mode gain and CMRR of the system. The input of both AE were connected together and 1.6 V_{p-p} sinusoidal signal with a DC offset of 2 V was applied from the function generator and the output of both AE was connected to the channel 2 of ADS1299 EVM.*

3.4.3 Frequency Response

The frequency response defines the active region of the system over a frequency range. As the system is intended to operate in the bandwidth of 262 Hz, thus the frequency response test was employed from 0.05 Hz to 500 Hz. A 20 mV_{P-P} sinusoidal signal with 2.5 V_{DC} offset from signal generator was given as input to the AE+ while the AE- was connected to 2.5 V from battery circuit. The output of AE+ and AE- was connected to the channel 2 of ADS1299 EVM as illustrated in the Figure 21. The gain was adjusted to 24, and the output signal was recorded in ADS1299 EVM software. The frequency response curve was later calculated in the MATLAB software.

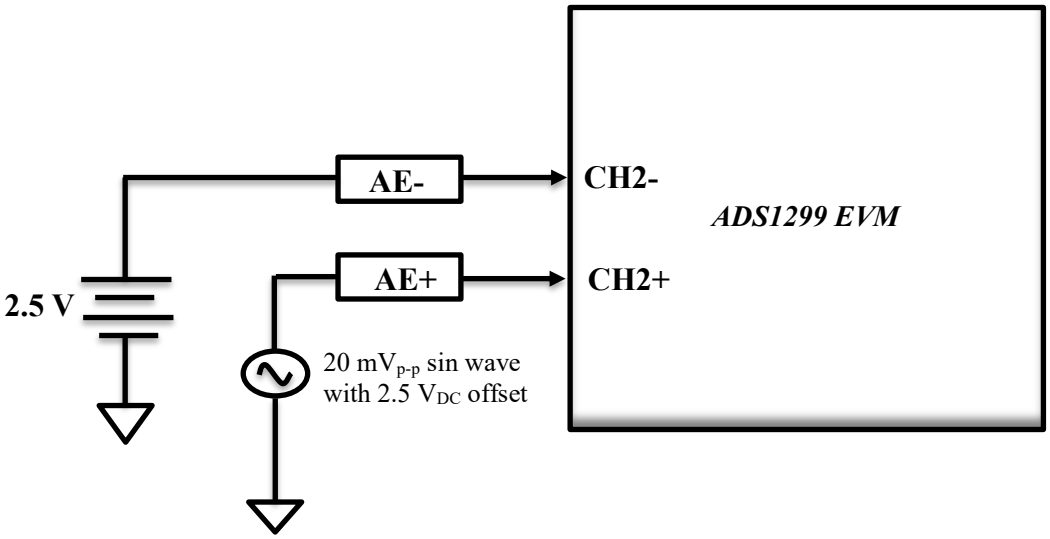

Figure 21. *Measurement setup for the frequency response of the system. The input signal ranges from 50 mHz to 500 Hz.*

3.5 ECG Measurement

The performance of the developed ECG system was carried out with the BioNomadix wireless system module BN-RSPEC presented in Figure 22 and BioPac MP160. This test was also carried out to evaluate the performance of these devices for recording QRS complexes and P waves for shortest IED around the heart main axis. The measurement was performed in the Health and Assistive Technology (HEAT) lab which is a joint venture of Tampere University of Technology (TUT) and Tampere University of Applied Sciences (TAMK). The HEAT lab is located in TAMK. The measurement was performed on one 30 years old male having BMI of 30.9. The measurements were divided into two parts. First, a large distance between electrodes was employed, and later the best electrode pair around the heart main axis was evaluated with shorter IED. Following sections describe the settings for these two measurements in details.

3.5.1 Measurement Setup

Both systems were checked separately before connecting those in the subject. After checking the performance of each system, then both systems were attached to the subject. The ECG channel from the BN-RSPEC transmitter module was utilized only while the RSP channel was turned off. The BN-RSPEC transmitter has the fixed gain of 2000, and

the differential input impedance is 2 M Ω as mentioned in Table 5. The gain of the ADS1299 system was set to 24, and channel 2 was used in the measurement. The sampling rate of ADS1299 was set to 1000 SPS to record ECG in desired bandwidth while 2000 SPS was set by AcqKnowledge as preset. Each lead measurement for the BN-RSPEC was taken for 30 seconds while ADS1299 system recorded for 10 seconds.

Each lead was recorded separately to the devices thus one lead was connected to AE+ and AE- while a separate proximate lead was connected to the BN-RSPEC module at the same time. Although the bias or ground electrode can be placed anywhere in the body but conventionally it is placed on the right side of the abdomen [58]. In this measurement, the bias electrode from ADS1299 was connected to the upper right abdomen, and the GND electrode from BN-RSPEC transmitter was connected to lower right abdomen of the subject. Both active electrodes and ADS1299 was powered from two separate single supply. The supply voltage for AE+ and AE- was taken from two coin cells battery, and ADS1299 was powered from a 6V battery power supply. The BN-EL30-Lead3 which has 30 cm long three cables was used in this measurement to connect both system to the subject. The key characteristics of these two systems is listed in the Table 5,

Table 5. *Main characteristics of both systems [57, 59]*

Parameters	**AE+ADS1299**	**BN-RSPEC Module + MP160**
Bandwidth (Hz)	0-262	0.05-150
Gain	24	2000
Sampling Rate (Hz)	1000	2000
Input Impedance (Ω)	10 T	2M
CMRR	109 dB	110 dB
Noise Voltage (μV_{pp})	2.76	2.54
Input Voltage Range (mV_{pp})	375	10
ADC Resolution (Bit)	24	16
ENOB	18.85	12

ADS1299 EVM and AcqKnowledge software were used to record ECG. No additional filters and analyzing tools from these software were utilized in the recording. The recorded signal from the AcqKnowledge software was saved as a .mat format to evaluate in the MATLAB. Similarly, the recorded signal from the ADS1299 EVM was analyzed in the MATLAB.

Figure 22. *BN-RSPEC Transmitter and Receiver Module [59].*

3.5.2 Measurement for long IED

In this measurements, electrodes were placed diagonally along the heart main axis. The largest distance between the electrodes was 23 cm, and the shortest distance was 8.5 cm. Ambu® Blue Sensor P-type electrode was used in this measurement. The electrodes placement used in this measurement is demonstrated in Figure 23 (left). The electrodes are placed along the heart main axis by centering the standard precordial lead V2. The distances between the electrodes in bipolar lead used in this measurement are presented in Table 6. This test was performed to evaluate the effect of electrodes proximity in bipolar measurement.

Table 6. *Electrode Distance for long distance measurement*

Lead	Distance (in cm)
1-5	23
2-5	18
3-5	13
4-5	8.5

3.5.3 Measurement Short IED

The measurement was performed to evaluate the shortest possible IED for bipolar measurement with acceptable SNR. The electrodes was placed according to the findings of Puurtinen [5]. The P wave was targeted mainly in this measurement as it easily lost under the noise. The bipolar lead 1-2 and 3-4 is placed near the sternum and the lead 5-6 near to right ventricle where electrode 5 is standard precordial lead V2. Ambu® Blue Sensor N electrode was used in this measurement. The electrode arrangement is illustrated in the right part of Figure 23. Two different IED was used in this measurement for lead 1-2 and 3-4 only one IED for the lead 5-6. The largest distance between the electrodes was 4.5 cm and the lowest distance was 0.2-0.3 cm. The electrode distance used in this measurement is given in Table 7. Overall this test evaluates the effect of electrodes proximity in bipolar measurement.

Table 7. *Electrode Distance for short IED measurement*

Lead	Distance (in cm)
1-2	4.5
1-2	0.2-0.3
3-4	4.5
3-4	0.2-0.3
5-6	5.5

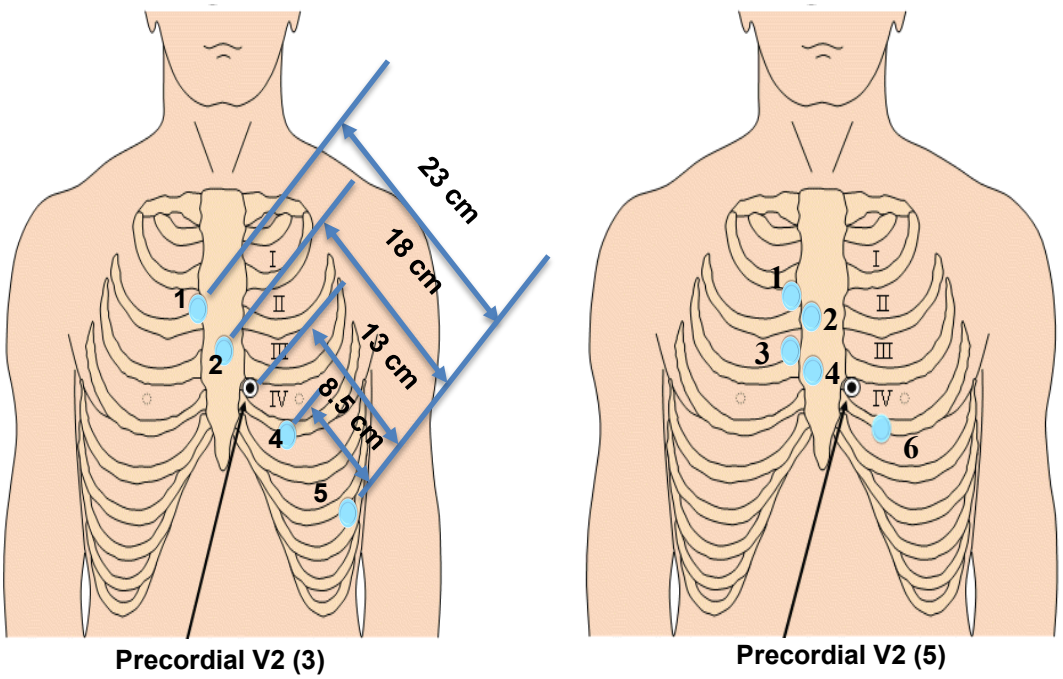

Figure 23. *Electrode Setup for long IED (left) and short IED (right) modified from [6].*

4. EXPERIMENTAL RESULTS

A brief discussion about the accomplished worked, and measurement results are presented in this chapter. A small description about the developed AE is given in section 4.1. Later in section 4.2, the electrical test results from the system are presented. Finally, the results from simultaneous measurement are given in section 4.3

4.1 Active Electrode

The design and assembly of the AE was the most time-consuming part of this thesis. Initially, two different AE designs were implemented, but later only the OPA2140 based AE was included in the measurement due to noise performance. As the low noise performance is expected thus PCB design and assembly was done with special care. The PCB layout of AE is given in Appendix A. The cable length of the system is kept as small as possible to reduce the coupling effect and movement artifact. The total dimension of this prototype AE is around 40 mm.

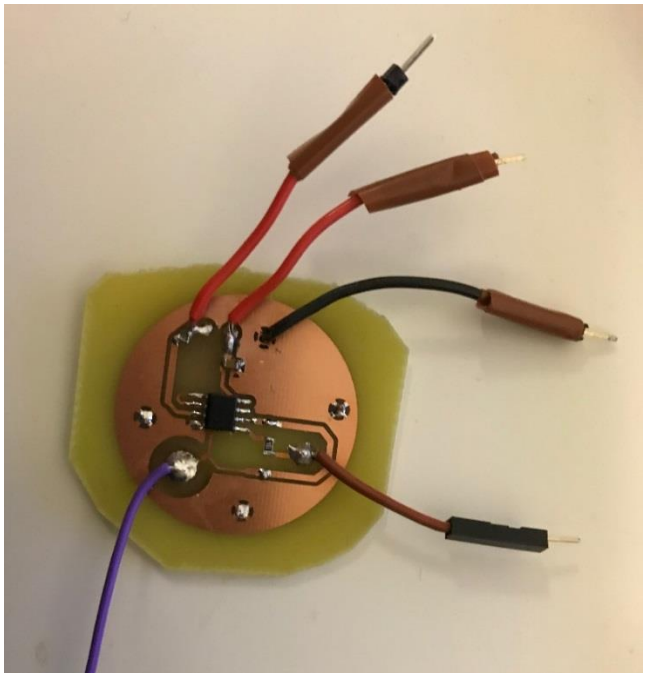

Figure 24. *Active Electrode.*

4.2 Measurement System

The measurement system consisted of two AE and one ADS1299 EVM. The output from the electrodes were connected to the AE's input and the output of the AE was connected to the channel 2 input of EVM.

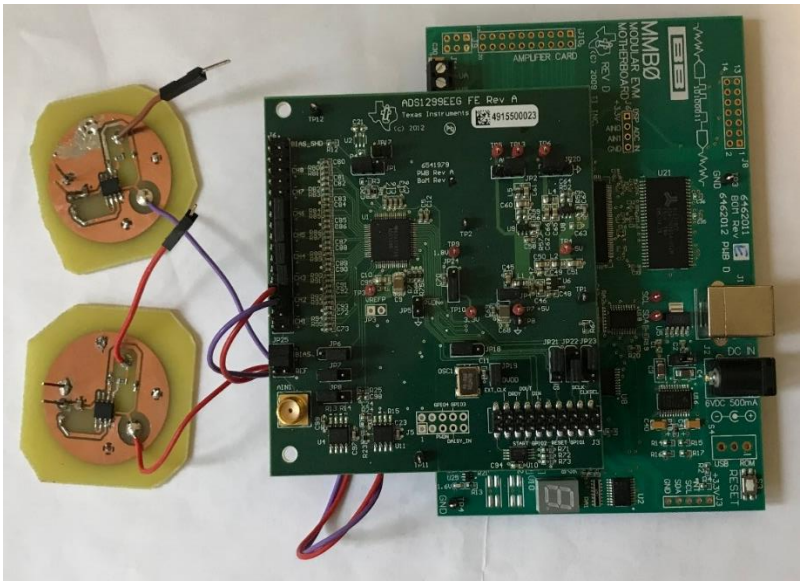

Figure 25. *ECG Measurement System.*

4.3 Electrical Tests

These sections describe the measurement results that were conducted to evaluate the performance fully operational ECG measurement system as the setup mentioned in section 3.6.

4.3.1 Noise

The calculated thermal noise of the system is shown in Table 8. It can be seen that the primary source of the noise is coming from the ADS1299 and the protection resistors. The noise contributed by the op-amp is much lower, and the maximum noise comes from the voltage noise thus only voltage noise is shown in the Table 8. The total noise of the system is 2.17 μV_{PP} or 0.76 μV_{RMS}.

Table 8. *The calculated thermal noise of the system at room temperature (25°C).*

Protection Resistors (μV_{PP})	Op Amp (E_N) (μV_{PP})	Anti-Aliasing Filter (μV_{PP})	ADS1299 (μV_{PP})	Total Noise (μV_{PP})
0.82	0.4	0.18	1.97	2.17

The measured noise test slightly differs from the calculated value which is shown in Table 9. The recorded signal contained a DC offset of 24 µV which was removed by subtracting the mean from the recorded data. This subtraction was done in the MATLAB. The system shows an excellent noise property over the desired frequency range. The output data rate was chosen to 1000 SPS so that the ENOB of the ADC remains high to maintain the good SNR. The recorded IRN of the system is also shown the Figure 26.

Table 9. *The measured and the calculated noise of the system in μV_{PP}*

Output Data Rate (SPS)	3-dB Bandwidth	Calculated Noise (μV_{PP})	Measured Noise (μV_{PP})	Difference (μV_{PP})
1000	262	2.17	2.76	0.59

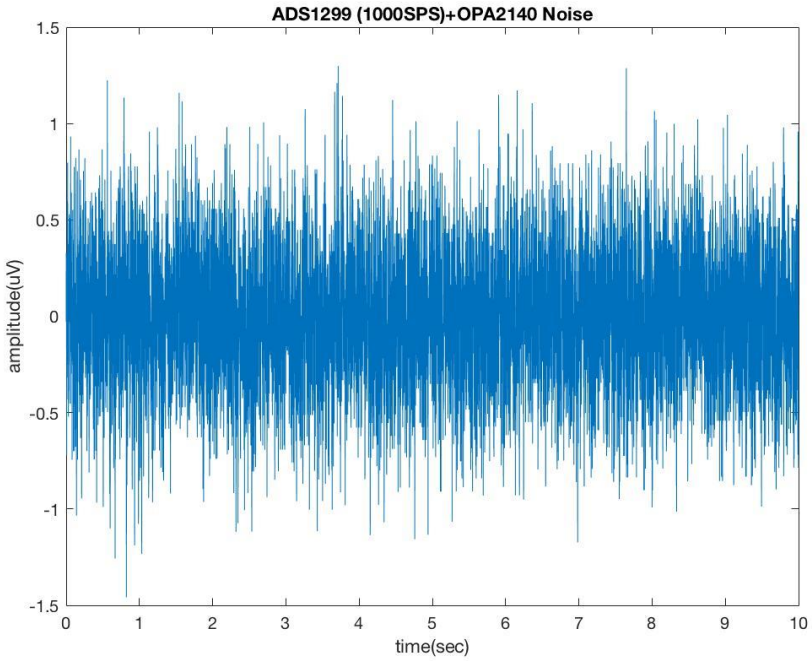

Figure 26. *Measured IRN of the measurement system*

4.3.2 CMRR

According to the Table 10, the CMRR of the system is -109 dB at 50 Hz which is quite similar to the datasheet value. Although ADS1299 provides the bias feedback option for improving the CMRR by applying a negative feedback to the human body as mentioned in the 3.5.3 but this test was performed to evaluate the minimum possible CMRR that can be employed by the ADS1299.

Table 10. *CMRR of ECG measurement System*

Frequency	V_{cm} (V_{pp})	V_{OUT} (μV_{pp})	Calculated CMRR (dB)	CMRR from Datasheet (dB)
50 Hz	1.6	135.65	-109	-110 to 120

4.3.3 Frequency Response

The frequency response of the system is specified in Figure 27. The upper -3 dB point is 262 Hz which is similar to the specified value in the datasheet of ADS1299 [57]. The lowest frequency was provided 50 mHz.

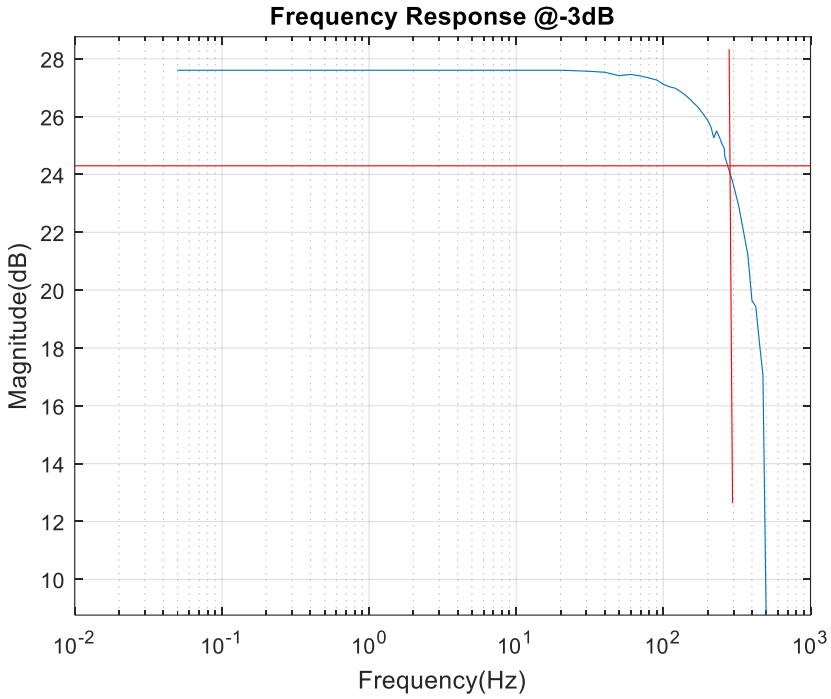

Figure 27. *Frequency Response of the measurement system. The upper cut-off frequency of the system is 262 Hz.*

4.4 Comparison Test

The simultaneous measurement with BN-RSPEC mentioned in section 3.7 is discussed briefly in this section. The following sections are divided into two parts: section 4.3.1 illustrate the results for longer IED measurement along the heart axis whereas section 4.3.2 demonstrate the results for the short IED measurement near the right atrium (standard precordial V2).

4.4.1 Long IED along Heart Main Axis

In this section, the signal strength was evaluated for the bipolar lead for longer IED along heart main vector. This test was also implemented to assess the performance of the AE+ADS1299 system as well as the BN-RSPEC module. The electrical activity of the

heart can be detected with high accuracy along heart axis which is reflected in the results of Table 11. The SNR values for QRS complexes for different IED demonstrate the performance of these devices. The SNR remains same for the QRS complex that lies within the main axis. If the lead lies within the heart axis the SNR for the QRS complex reduced by 4 dB for the AE+ADS1299 system whereas the SNR of the BN-RSPEC is reduced by 9 dB. The SNR for P wave is also reduced in both devices depending on the location and IED. The summary of these measurements are presented for as SNR both devices in Table 11.

Table 11. *SNR of both system for IED 4-23 cm*

Lead	AE+ADS1299		BN-RSPEC Module + MP160	
	P wave (dB)	QRS (dB)	P wave (dB)	QRS (dB)
1-5	34	59	33	58
2-5	33	58	32	57
3-5	24	58	25	56
4-5	21	55	22	49

It can be seen that SNR reduces with the increase in electrode proximity. Moreover, Table 11 shows that the lead 1-5 has the highest SNR compared to the lead 4-5. The reason is that the electrode distance was larger in 1-5 and it covered the entire heart while the lead 4-5 situated one side of the heart and it recorded only the electrical activity of that location. In this lead location, the signal strength of P wave is lower thus the SNR is lower. The difference in the frequency range between the devices also reflects in the SNR. The AE+ADS1299 system provides a high SNR compare to BN-RSPEC module as the ENOB of ADS1299 is 6 bit higher [57, 59].

Figure 28 show the recorded signals amplitude and morphology for the IED between 8.5 cm to 23 cm. Signals from both devices were processed in the MATLAB and only the mean value was subtracted from the recorded signal of the AE+ADS1299 system. The signals from the BN-RSPEC module is the raw signal which was converted to µV scale to represent in the same scale. The sampling rate of BN-RSPEC was also down-sampled to 1000 Hz in MATLAB to represent in the same scale. The signals presented in Figure 28 are similar to the standard Lead II as the leads lie in the heart's main axis. The proximal electrodes reduce the signals shape of the P wave drastically and which are barely recognizable.

The highest amplitude for P wave was found in the lead 1-5 and 2-5 electrode pair for both devices. The highest amplitude was approximately 125 μV for AE+ADS1299 system whereas the BN-RSPEC recorded highest P wave was approximately 102 μV. The lowest amplitude for P wave was found in 4-5 lead for both device. The amplitude was less than 31 μV for both device.

The highest value for QRS complex was also found in 1-5 lead pair for devices on the other hand the lowest value was observed in 4-5 lead. The recorded value in BN-RSPEC module is lower compared to AE+ADS1299 as expected which is due to the difference in frequency range and dynamic range of both system.

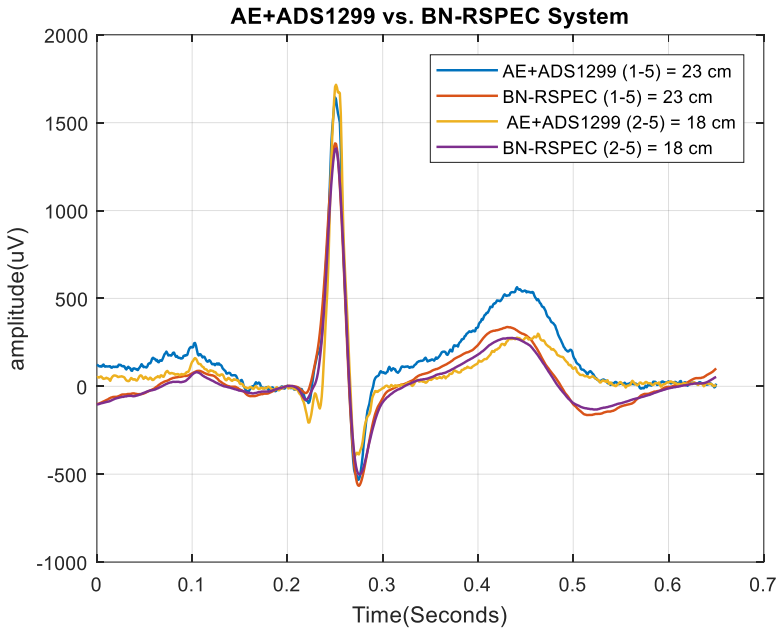

(a)

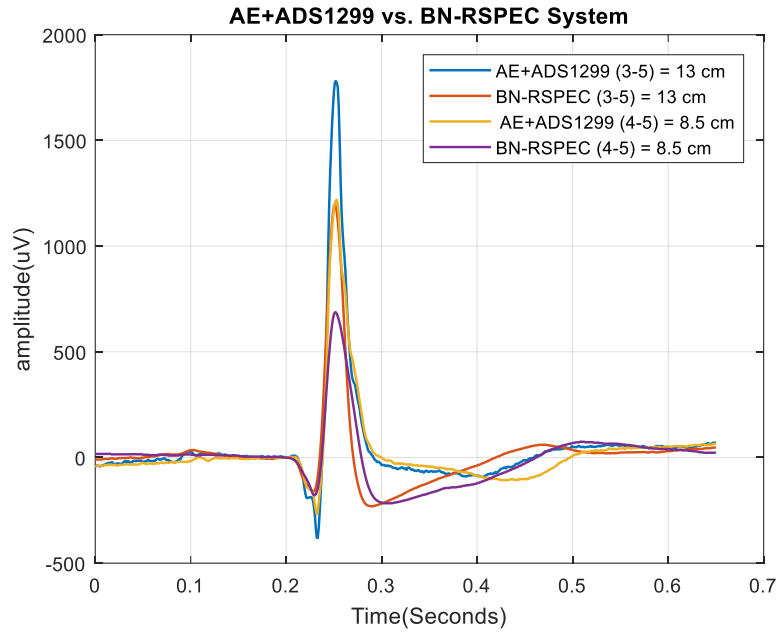

(b)

Figure 28. *In this measurement, Blue Sensor P electrode having sensing area of 10 mm^2 was used. The frequency range for AE+ADS1299 was 0-262 Hz whereas BN-RSPEC was 0.05-150Hz.* ***(a)*** *ECG recording for lead 1-5 and 2-5 where IED was 23 cm and 18 cm respectively. The signal strength of P wave, the QRS complex and the T wave is much prominent for both devices.* ***(b)*** *The QRS complex is larger in AE+ADS1299 than BN-RSPEC system for lead 3-5 and 4-5 (IED 13 cm and 8.5 cm respectively). The strength of P wave was reduced due to the measurement location and reduced IED.*

4.4.2 Short IED near Right Atrium

Both devices are capable of capturing P wave even in short distance less than 0.3 cm as both devices have small noise level. But the P wave can lost under the noise, and it is strongly dependent on the location of the electrodes.

Table 12 is presented with SNR for short IED where the lead 1-2 and lead 3-4 were closer to the right atrium and lead 5-6 was closer to right ventricle. The minimum distance between the electrodes was 0.2-0.3 cm while the maximum distance was kept 4.5 cm for lead 1-2 and lead 3-4. Lead 5-6 was recorded with IED of 5.5 cm. It can be seen that even with this short distance between the electrodes, the P waves are distinguishable. If the SNR of P wave from Table 11 and Table 12 are compared together, then it is visible that the strength of P wave for the lead 4-5 (IED = 8.5 cm) was similar to the lead 1-2 and lead 3-4 where the IED was less than 0.3 cm for the AE+ADS1299 system. The BN-RSPEC module showed a lower SNR compared to the AE+ADS1299 system because of the difference in frequency range and the ADC resolution in both system.

Table 12. *SNR of both system for short IED 0.2-5.5 cm*

Lead	Distance (cm)	AE+ADS1299		BN-RSPEC Module + MP160	
		P wave (dB)	QRS (dB)	P wave (dB)	QRS (dB)
1-2	4.5	28	50	26	49
1-2	0.2-0.3	21	40	17	39
3-4	4.5	32	54	29	53
3-4	0.2-0.3	21	45	19	42
5-6	5.5	27	56	26	54

Similar to the previous measurement, the signals in Figure 29 were analyzed in MATLAB. As the electrode distance is much closer to each other thus, this measurement showed a prominent shape of the signals. The signal morphology changes also depending on the location of the leads. Lead 1-2 and lead 3-4 are similar to the standard precordial V2 while lead 5-6 is similar to the V3 as the previous leads are more near to the atria while lead 5-6 is near to right ventricle. Thus the local activity of these locations is noticeable even with the short distance of 0.2-0.3 cm. The P wave and the T wave are in same phase where the QRS complex is in opposite direction for lead 1-2 and 3-4. Alternatively, the P wave, QRS complex and T wave are in the same phase for lead 5-6 which is similar to the standard precordial V3 lead.

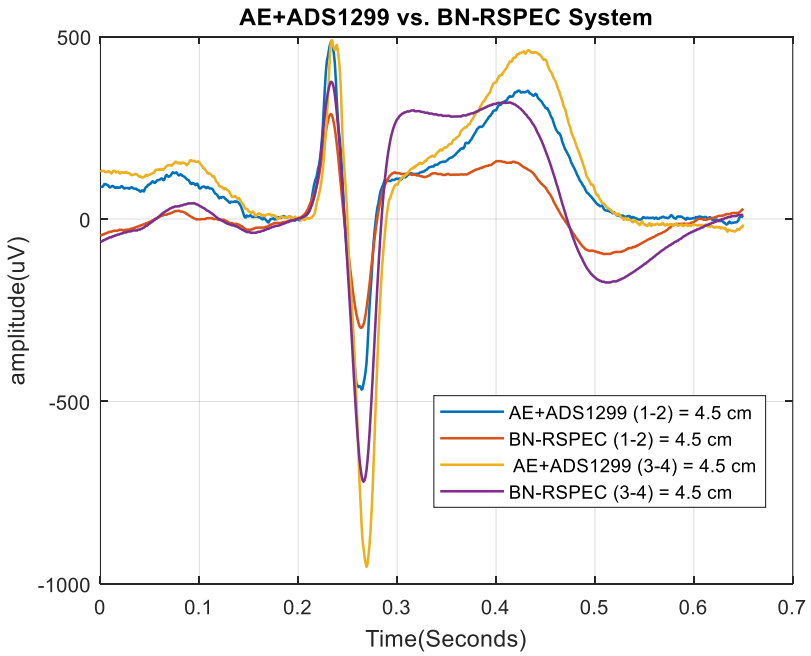

(a)

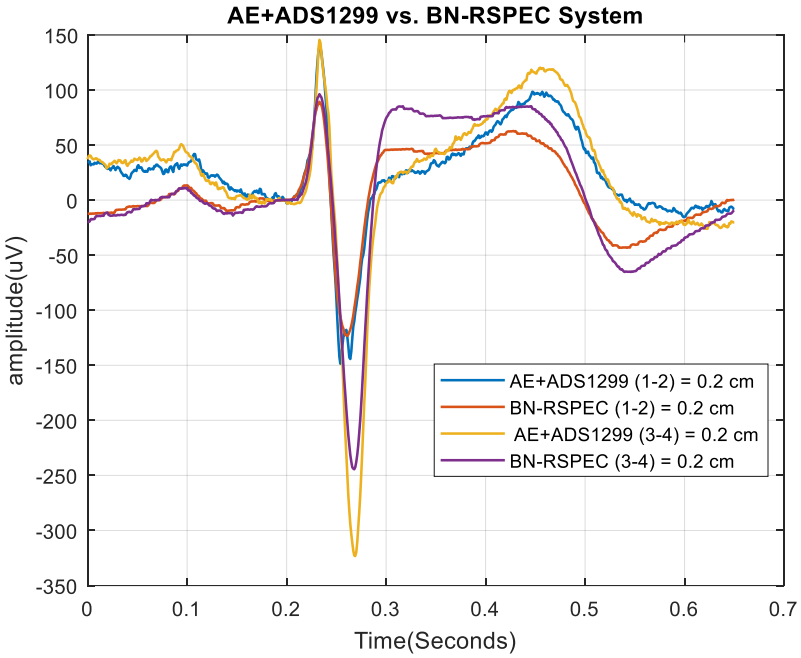

(b)

Figure 29. *The electrical activity of this measurement were recorded with Blue Sensor N having the sensing area of 15 mm^2. The signal strength varies depending on the measurement location and the IED. For* ***(a)*** *IED = 4.5 cm and* ***(b)*** *IED = 0.2-0.3 cm, the P wave and the QRS complex increased from lead 1-2 to lead 3-4 in both devices.*

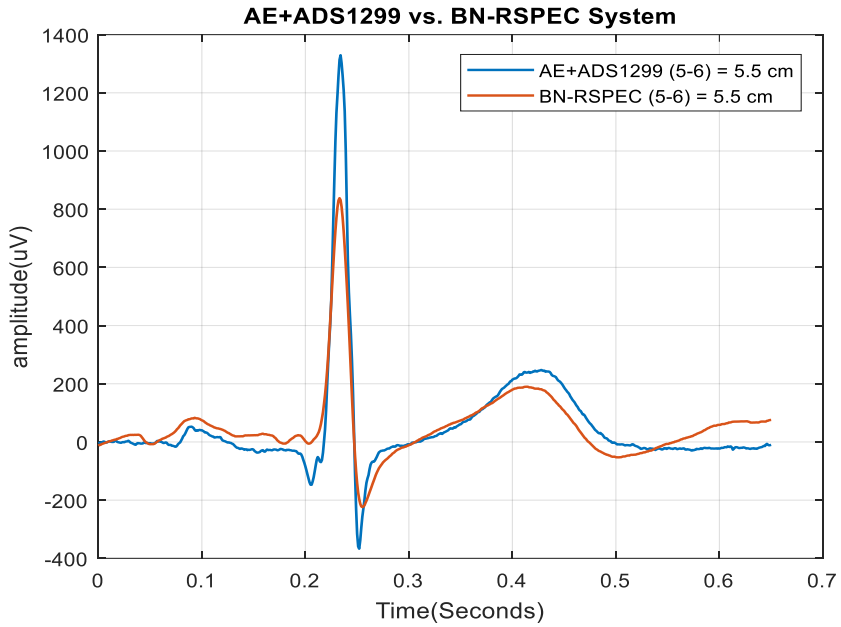

Figure 30. *The electrical activity of lead 5-6 where the IED = 5.5 cm. This measurement was recorded with Blue Sensor N electrode.*

If Figure 29 (a) and Figure 29 (b) are observed for P wave, then it can be seen that both AE+ADS1299 and BN-RSPEC systems are capable of recording of P wave lower than 40 µV even for short IED of 0.3 cm. Although the signal quality for P wave suffers greatly for BN-RSPEC module compared to AE+ADS1299 system due to the ADC resolution and frequency range as mentioned earlier. In Figure 29, the amplitude of P wave increases in the lead 3-4 than the lead 1-2 as the lead 3-4 is much nearer to the heart.

The QRS complex also reduced for both system in short IED. Similarly, when the leads are close to the heart then the amplitude of QRS complex gets stronger which is visible in Figure 29 and Figure 30 for the lead 3-4 and the lead 5-6 respectively. The QRS complex is prominent in the lead 5-6 although the distance between the electrodes was 5.5 cm.

5. DISCUSSION AND FUTURE WORK

The discussion about the findings, results, limitations and possibilities to improve and application of the current design will be provided in this sections.

The miniature electronics open the door for new kinds of physiological wearable systems. With the advancement of miniaturization, it is now possible to design physiological systems into a smaller unit. The wearable ECG devices are gaining attention as it can monitor for a long time and moreover, the absence of cable offers more comfort. These kind of devices are suitable for monitoring patients from their home especially the older adults.

The purpose of this thesis was to develop a wearable ECG system that can measure from the small bipolar lead from the chest. According to Puurtinen [5], the performance of the system depends on the electrode location and orientation as mentioned in section 2.4. Thus the performance of this system was evaluated from different locations of the chest with diagonally placed leads with different IED. The signal quality along with the signal morphology alters significantly depending on the locations of the lead as well as the IED. The next section will discuss the effect of measurement location findings from the result obtained in this thesis in details.

5.1 Measurement Location

The measurement location has a critical role in small wearable ECG system. The device can be placed on the chest to get good signal quality as well for the less movement artifact compared to the limb leads. It can be seen from the results that P wave was detectable distinguishably from the noise near the right atrium even with a short IED of less than 0.3 cm while the P wave was lost under noise in measurement from the left part of the thorax even with larger IED. These results also agree with the findings from the previous researches mentioned in section 2.4 [33, 43-45, 47, 48, 60, 61]. Similar results were obtained by Janata et al. [45] with the prototype from Philips Medical Systems. They also found the presence of P wave in mid-sternal location. The results also agree with the findings obtained by Puurtinen et al. [17]. Their finding indicates that the best location for detecting P was above the precordial leads V1 and V2.

5.2 Inter-Electrode-Distance

For a small wearable device it is necessary to place the electrodes as close as possible. The proximity of electrodes reduce the SNR radically. The effect of close bipolar lead in AE+ADS1299 system was also evaluated in this thesis. Based on the result it was observed that AE+ADS1299 is capable of recording ECG with acceptable SNR even with the distance less than 0.3 cm. The SNR for P wave with this IED was found 21 dB near

mid-sternum area. This distance was extremely small compared to the findings from other studies. The lowest IED was found to be 2.48 cm where the presence of P wave was obtained with an accuracy to 94-98 % [45]. Another study reflects the acceptable signal quality with a short IED of 3 cm [62]. Puurtinen et al. also found the strong ECG quality with a short IED of 5-6 cm although the dataset was used in this study was recorded before 1997 [17, 63]. Thus this developed system has great potential to develop as a single unit for wireless or portable device and can also be developed for clinical use.

5.3 Active Electrode

The single supply DC coupled AE showed an excellent noise performance over the desired frequency range. Moreover, the impedance imbalance introduced by the unprepared skin was reduced by the AE. As the subject was potentially driven by the ADS1299 thus single supply design was introduced. The operating voltage range of AE was 0.2V~3.1V even with this narrow range no saturation was observed in the ECG signal. The less component used in this AE make it suitable for application when larger bandwidth is needed due to the acceptable CMRR in higher frequency. Moreover, this AE is suitable for real time acquisition system as no HPF was used which introduce delay in the measurement. The main drawback of AE was that it crossed the standard safety current limit introduced by the AAMI [8].

5.4 The Measurement System

The high resolution DC coupled system demonstrated outstanding performance due to low noise and high CMRR. Although the IRN of the system differed from the calculated value but this value was much lower than the standard limit introduced by AAMI [8]. The bandwidth of the system was found to be similar to the datasheet value. The specification of this developed system is compared with different standards such as AHA and AAMI is presented in Table 13. It can be said that all requirement are fulfilled as this requirement was introduced long ago.

AC coupled measurement is necessary for 16 bit ADC. In this case, the HPF is essential to remove the DC offset. The 24 bit ADC can overcome this problem as the input voltage range is much higher compared to 16 bit ADC for the same resolution. The cut off frequency of HPF need to be chosen in such way that it cannot distort low frequency component such as ST-segment [64]. Furthermore, the components of the HPF reduce system CMRR, increase noise and introduce delay in the system.

Table 13. *Comparison between Standard and the Developed System*

Specification	AE+ADS1299	Standard [8, 12, 42]
Bandwidth (Hz)	0-262	0.67-150
Sampling Rate (Hz)	1000	500
Input Impedance (Ω)	10 T	2.5 M
Noise Voltage (μV_{pp})	2.76	30
Input Voltage Range (mV_{pp})	375	5
ADC Resolution (Bit)	24	8
ADC Quantization Noise (μV_{pp})	0.022	10

5.5 Comparison with BN-RSPEC Module

The main difference between the BN-RSPEC module+MP160 and the AE+ADS1299 system is the difference of ADC resolution, input impedance and frequency range. Due to the 24 bit ΔΣ ADC of ADS1299, it can record DC coupled signal, thus the system has low gain PGA. Moreover, AE+ADS1299 has high input impedance. On the other hand, BN-RSPEC module+MP160 has 16 bit ADC so that the maximum input voltage range is only 10 mV_{pp} to maintain low quantization noise of the system. Thus AC coupled signal with large gain is essential for this system. The input impedance of the system is much lower compared to AE+ADS1299 system. Furthermore the ENOB is also lower for this system. Although lower cutoff frequency of this system is 0.05 Hz it was observed that baseline was more shifted compared to the AE+ADS1299 system for short IED. Furthermore, the high SNR was observed in developed system in most cases due to the difference in ADC resolution and higher cutoff frequency. Although small SNR was also observed in the developed system in P wave of the lead 3-4 and the lead 4-5 for long IED measurement.

AE+ADS1299 system record P wave with high SNR for short IED less than 0.3 cm. The baseline is effected in BN-RSPEC module.

5.6 Limitation

All measurements in this thesis was performed on a single subject. Moreover, the active electrodes were connected to the body as well to the ADS1299 EVM with cable. Thus all experiments were done in sitting positions to minimize the movement artifact. Furthermore, ADS1299 and BN-RSPEC has different electrical and measurement characteristics thus it was not possible to compare them in greater extent.

5.7 Future Work

As the system showed a significant result even with the short IED, in the future work development of all the electronics and electrodes may be possible in a single unit. Furthermore, the performance of this system can be evaluated with dry electrodes as well. The short bipolar lead offers a new opportunity to detect the more local activity of the heart rather than the whole view of the heart detected by the standard 12-lead system or Holter monitor. Thus the performance of this system also can be evaluated on a larger population. Additionally, this system is capable of detecting P wave with high accuracy in sternum area thus it can be used in clinical evaluation.

6. CONCLUSIONS

This thesis is mainly focused on the development of small ECG system for the wearable application dedicated to the chest area. The implementation was started with the literature review where particular attention was given to the small wearable system development. The literature review was followed by a technical review, measuring system and the clinical evaluation of the previously developed system.

After considering the findings and the drawbacks of these research, the new design for the system was implemented. During the designing process, low noise electronics, number of components and ΔΣ ADC architecture were given priority to increasing the SNR and CMRR. AE was introduced in the design to reduce the motion artefact, screen preparing problem, and the power line interference. The AE was designed with a protection resistor and a high precision JFET Op Amp, OPA2140. This Op Amp is suitable for low noise application which is essential for short IED ECG device. The next part of the design considered the medical AFE, ADS1299 by Texas Instruments which incorporates a low noise PGA and ΔΣ ADC. The gain of the system is very small due to the ΔΣ ADC architecture thus dc coupling solution was utilized in this design which allows keeping the low frequency components of the ECG. In this thesis, instead of the AFE, an evaluation board of ADS1299 AFE was used to study the performance of this AFE for small ECG system. The ADS1299 EVM also offer evaluation software to control the register of the AFE from Microsoft Windows 7 PC.

The next part was to test the performance of AE+ADS1299 EVM system particularly the noise performance, CMRR and the frequency response. After getting satisfactory results, the next target was to find the capability of this system for short bipolar lead ECG measurement. To find the system's capability two types of measurement were executed: one with the diagonally placed electrodes with larger IED and another with the diagonally placed electrodes with the short IED. The measurement was simultaneously performed with BN-RSPEC module from Biopac Systems.

The results showed that the developed system outperforms the BN-RSPEC module in signal quality even with the short electrode distance due to differences in ADC resolution. The noise performance of the developed system is excellent and very much suitable for small wearable ECG application. The P wave and the QRS complex can be measured with acceptable SNR by the developed system even with the short IED.

The significant outcomes from these measurements were that the measurement location on the chest plays a critical role. It is also evident from the results that the best location for detecting the P wave was found near the mid-sternum area specifically in the precordial V2 lead which agrees with the finding from the previous research. Another significant

finding was that both systems were capable of detecting P wave and QRS complex in short electrode distance less than 0.3 cm although AE+ADS1299 system outperforms the BN-RSPEC module.

Form the results it can be said that the AE+ADS1299 AFE is suitable for wearable application specifically for short IED wearable device for chest.

REFERENCES

[1] Betts J. Gordon, Desaix Peter, Johnson Eddie, Anatomy and Physiology, OpenStax College, Houston, TX: OpenStax CNX, 2013, 823-855 p.

[2] WHO Cardiovascular diseases (CVDs), World Health Organization, web page. Available (accessed 22/
05): http://www.who.int/news-room/fact-sheets/detail/cardiovascular-diseases-(cvds).

[3] M. AlGhatrif, J. Lindsay, A brief review: history to understand fundamentals of electrocardiography, Journal of community hospital internal medicine perspectives, Vol. 2, Iss. 1, 2012, pp. 1-5. http://www.ncbi.nlm.nih.gov/pubmed/23882360.

[4] H.L. Kennedy, The History, Science, and Innovation of Holter Technology, Annals of Noninvasive Electrocardiology, Vol. 11, Iss. 1, 2006, pp. 85-94. http://www.ingenta-connect.com/content/bsc/anec/2006/00000011/00000001/art00016.

[5] M. Puurtinen, Precordial Bipolar Leads for Mobile ECG Applications, Tampere University of Technology, 2012, Available: https://tutcris.tut.fi/portal/en/publications/precordial-bipolar-leads-for-mobile-ecg-applications(98638e58-6f26-4165-bb57-98b7f43ffc04).html.

[6] J. Malmivuo, R. Plonsey, Bioelectromagnetism, Oxford Univ. Press, New York, 1995.

[7] L. Sörnmo, P. Laguna, Bioelectrical signal processing in cardiac and neurological applications, Elsevier Acad. Press, Amsterdam [u.a.], 2005, 411-428 p.

[8] M.R. Neuman, J. Webster, Biopotential Electrodes, Medical instrumentation: Application and Design, 4th ed. John Wiley & Sons Inc, Hoboken, N.J, 1997.

[9] R. Trobec, I. Tomasić, A. Rashkovska, M. Depolli, V. Avbelj, Body Sensors and Electrocardiography, 1st ed. 2018 ed. Springer Verlag, Cham, 2017.

[10] Jari Hyttinen, Development of Regional Aimed ECG Leads Especially for Myocardial Ischemia Diagnosis, Tampere University of Technology, 1994, Available: http://www.bem.fi/edu/doctor/hyttinen/.

[11] Abächerli, Roger, PhD|Schmid, Hans-Jakob, MSE, Meet the challenge of high-pass filter and ST-segment requirements with a DC-coupled digital electrocardiogram amplifier, Journal of Electrocardiology, Vol. 42, Iss. 6, 2009, pp. 574-579. https://www.clinicalkey.es/playcontent/1-s2.0-S0022073609003240.

[12] P. Kligfield, L.S. Gettes, J.J. Bailey, R. Childers, B.J. Deal, E.W. Hancock, G. van Herpen, J.A. Kors, P. Macfarlane, D.M. Mirvis, O. Pahlm, P. Rautaharju, G.S. Wagner, Recommendations for the Standardization and Interpretation of the Electrocardiogram: Part I: The Electrocardiogram and Its Technology: A Scientific Statement From the

American Heart Association Electrocardiography and Arrhythmias Committee, Council on Clinical Cardiology; the American College of Cardiology Foundation; and the Heart Rhythm Society Endorsed by the International Society for Computerized Electrocardiology, Circulation, Vol. 115, Iss. 10, 2007, pp. 1306. http://circ.ahajournals.org/cgi/content/abstract/115/10/1306.

[13] J.J. Bailey, A.S. Berson, J. Garson A, L.G. Horan, P.W. Macfarlane, D.W. Mortara, C. Zywietz, Recommendations for standardization and specifications in automated electrocardiography: bandwidth and digital signal processing. A report for health professionals by an ad hoc writing group of the Committee on Electrocardiography and Cardiac Electrophysiology of the Council on Clinical Cardiology, American Heart Association, Circulation, Vol. 81, Iss. 2, 1990, pp. 730-739. http://www.ncbi.nlm.nih.gov/pubmed/2297875.

[14] E William Hancock, Barbara J Deal, David M Mirvis, Peter Okin, Paul Kligfield, Leonard S Gettes, AHA/ACCF/HRS Recommendations for the Standardization and Interpretation of the Electrocardiogram, Journal of the American College of Cardiology, Vol. 53, Iss. 11, 2009, pp. 992. http://www.ncbi.nlm.nih.gov/pubmed/19281932.

[15] Analog front-end design for ECG systems using delta-sigma ADCs, ECN-Electronic Component News, Vol. 54, Iss. 5, 2010, pp. 12.

[16] Bonnie Baker Delta-sigma ADCs in a nutshell, EDN, web page. Available (accessed website 05/05): http://www.rpi.edu/dept/ecse/rta/LMS/Delta-Sigma_ADCs.pdf.

[17] M. Puurtinen, J. Viik, J. Hyttinen, Best Electrode Locations for a Small Bipolar ECG Device: Signal Strength Analysis of Clinical Data, Annals of Biomedical Engineering, Vol. 37, Iss. 2, 2009, pp. 331-336. http://www.ncbi.nlm.nih.gov/pubmed/19020977.

[18] Myer Kutz, Standard handbook of biomedical engineering and design, The McGraw-Hill Companies, Inc., New York, 2003, .

[19] M. Fernandez, R. Pallas-Areny, A simple active electrode for power line interference reduction in high resolution biopotential measurements, Proceedings of 18th Annual International Conference of the IEEE Engineering in Medicine and Biology Society, Amsterdam, Netherlands, IEEE, pp. 98 vol.1.

[20] V. Acharya Improving Common-Mode Rejection Using the Right-Leg Derive Amplifier
, web page. Available (accessed 05/05): http://www.ti.com/lit/an/sbaa188/sbaa188.pdf.

[21] J.J. Carr, J.M. Brown, Introduction to biomedical equipment technology, 2nd ed. ed. Regents, Englewood Cliffs, 1993, .

[22] Li Jack Thermal Noise Analysis in ECG Applications, Texas Instruments, web page. Available (accessed 24/06): http://www.ti.com/lit/an/sbaa185/sbaa185.pdf.

[23] S. Franco, Design with operational amplifiers and analog integrated circuits, 2. ed., internat. ed. ed. McGraw-Hill, Boston, Mass, 1998.

[24] A. Cömert, The Assessment and Reduction of Motion Artifact in Dry Contact Biopotential Electrodes, Tampere University of Technology, 2015, Available: https://tut-cris.tut.fi/portal/en/publications/the-assessment-and-reduction-of-motion-artifact-in-dry-contact-biopotential-electrodes(011a3ab2-9cd4-4b6e-9cd5-e8518de14f50).html.

[25] J.G. Webster, Reducing Motion Artifacts and Interference in Biopotential Recording, IEEE Transactions on Biomedical Engineering, Vol. BME-31, Iss. 12, 1984, pp. 823-826. https://ieeexplore.ieee.org/document/4121779.

[26] J. Rosell, J. Colominas, P. Riu, R. Pallas-Areny, J.G. Webster, Skin impedance from 1 Hz to 1 MHz, IEEE Transactions on Biomedical Engineering, Vol. 35, Iss. 8, 1988, pp. 649-651. https://ieeexplore.ieee.org/document/4599.

[27] ØG. Martinsen, S. Grimnes, E. Haug, Measuring depth depends on frequency in electrical skin impedance measurements, Skin Research and Technology, Vol. 5, Iss. 3, 1999, pp. 179-181. https://onlinelibrary.wiley.com/doi/abs/10.1111/j.1600-0846.1999.tb00128.x.

[28] G. Medrano, A. Ubl, N. Zimmermann, T. Gries, S. Leonhardt, Skin Electrode Impedance of Textile Electrodes for Bioimpedance Spectroscopy, in: Anonymous (ed.), 13th International Conference on Electrical Bioimpedance and the 8th Conference on Electrical Impedance Tomography, Springer Berlin Heidelberg, Berlin, Heidelberg, 2007, pp. 260-263.

[29] A. Cömert, M. Honkala, J. Hyttinen, Effect of pressure and padding on motion artifact of textile electrodes, Biomedical engineering online, Vol. 12, Iss. 1, 2013, pp. 26. http://www.ncbi.nlm.nih.gov/pubmed/23565970.

[30] A. Cömert, J. Hyttinen, Investigating the possible effect of electrode support structure on motion artifact in wearable bioelectric signal monitoring, Biomedical engineering online, Vol. 14, Iss. 1, 2015, pp. 44. http://www.ncbi.nlm.nih.gov/pubmed/25976349.

[31] Tae-Ho Kang, C.R. Merritt, E. Grant, B. Pourdeyhimi, H.T. Nagle, Nonwoven Fabric Active Electrodes for Biopotential Measurement During Normal Daily Activity, IEEE Transactions on Biomedical Engineering, Vol. 55, Iss. 1, 2008, pp. 188-195. https://ieeexplore.ieee.org/document/4404089.

[32] W.H. Ko, Active electrodes for EEG and evoked potential, Proceedings of the 20th Annual International Conference of the IEEE Engineering in Medicine and Biology Society. Vol.20 Biomedical Engineering Towards the Year 2000 and Beyond (Cat. No.98CH36286), Hong Kong, China., IEEE, pp. 2224 vol.4.

[33] J.K. Russell PhD, S. Gehman BS, Early experience with a novel ambulatory monitor, Journal of Electrocardiology, Vol. 40, Iss. 6, 2007, pp. S164. https://www.ncbi.nlm.nih.gov/pubmed/17993315.

[34] R. Fensli, E. Gunnarson, O. Hejlesen, A wireless ECG system for continuous event recording and communication to a clinical alarm station, The 26th Annual International

Conference of the IEEE Engineering in Medicine and Biology Society, San Francisco, CA, USA, IEEE, pp. 2208-2211.

[35] M.C. Munshi, Xiaoyuan Xu, Xiaodan Zou, E. Soetiono, Chang Sheng Teo, Yong Lian, Wireless ECG plaster for body sensor network, 2008 5th International Summer School and Symposium on Medical Devices and Biosensors, Kranjska Gora, Slovenia, IEEE, pp. 310-313.

[36] Yishan Wang, R. Wunderlich, S. Heinen, Design and evaluation of a novel wireless reconstructed 3-lead ECG monitoring system, 2013 IEEE Biomedical Circuits and Systems Conference (BioCAS), Rotterdam, Netherlands, IEEE, pp. 362-365.

[37] A.A. Uddin, Development of an Ambulatory Wearable Sensor System for Behavioural Neurocardiac Training, ProQuest Dissertations Publishing, 2014, Available: https://search.proquest.com/docview/1650585299.

[38] Savvy Savvy Sensor, Monitor the activity of your heart. Anytime and anywhere. web page. Available (accessed 17/05): http://www.savvy.si/en/Buy/SAVVY-ECG_2/.

[39] R. Trobec, M. Depolli, V. Avbelj, Wireless network of bipolar body electrodes, 2010 Seventh International Conference on Wireless On-demand Network Systems and Services (WONS), Kranjska Gora, Slovenia, IEEE, pp. 145-150.

[40] iRhythm Technology Zio XT
, web page. Available (accessed 16/05): http://www.irhythmtech.com/products-services/zio-xt.

[41] Bardy Diagnostics Carnation Ambulatory Monitor™, web page. Available (accessed 16/05): https://www.bardydx.com/wp-content/uploads/2017/05/DWG00189B-BDx_CAM_RackCard.pdf.

[42] J L Willems, P Arnaud, J H van Bemmel, R Degani, P W Macfarlane, C Zywietz, Common standards for quantitative electrocardiography: goals and main results. CSE Working Party, Methods Archive, Vol. 29, Iss. 4, 1990, pp. 263-271. http://www.schattauer.de/de/magazine/uebersicht/zeitschriften-a-z/methods/contents/archivepremium/issue/1210/manuscript/14488/show.html.

[43] I.H. Hansen, K. Hoppe, A. Gjerde, J.K. Kanters, H.B.D. Sorensen, Comparing twelve-lead electrocardiography with close-to-heart patch based electrocardiography, 2015 37th Annual International Conference of the IEEE Engineering in Medicine and Biology Society (EMBC), Chicago, IL, USA, 26-30 Aug. 2014, IEEE, United States, pp. 330-333.

[44] M.E. Lemmert MD, A. Janata MD, P. Erkens MS, J.K. Russell PhD, S. Gehman BS, K. Nammi MS, Crijns, Harry J.G.M., MD, PhD, F. Sterz MD, Gorgels, Anton P.M., MD, PhD, Detection of ventricular ectopy by a novel miniature electrocardiogram recorder, Journal of Electrocardiology, Vol. 44, Iss. 2, 2011, pp. 222-228. https://www.clinicalkey.es/playcontent/1-s2.0-S0022073610005479.

[45] A. Janata, M. Lemmert, J.K. Russell, S. Gehman, R. Fleischhackl, O. Robak, E. Pernicka, F. Sterz, A.P.M. Gorgels, Quality of ECG Monitoring with a Miniature ECG Recorder, Pacing and Clinical Electrophysiology, Vol. 31, Iss. 6, 2008, pp. 676-684. https://onlinelibrary.wiley.com/doi/abs/10.1111/j.1540-8159.2008.01070.x.

[46] Ki Moo Lim, Jae Won Jeon, Min-Soo Gyeong, Seung Bae Hong, Byung-Hoon Ko, Sang-Kon Bae, Kun Soo Shin, Eun Bo Shim, Patient-Specific Identification of Optimal Ubiquitous Electrocardiogram (U-ECG) Placement Using a Three-Dimensional Model of Cardiac Electrophysiology, IEEE Transactions on Biomedical Engineering, Vol. 60, Iss. 1, 2013, pp. 245-249. https://ieeexplore.ieee.org/document/6263285.

[47] Barrett, Paddy M., MB, BCh, BAO, R. Komatireddy MD, Haaser, Sharon, RN, BSN, CCRC, Topol, Sarah, RN, BSN, BA, J. Sheard MPH, J. Encinas MS, A.J. Fought MS, E.J. Topol MD, Comparison of 24-hour Holter Monitoring with 14-day Novel Adhesive Patch Electrocardiographic Monitoring, American Journal of Medicine, The, Vol. 127, Iss. 1, 2014, pp. 95.e17. https://www.clinicalkey.es/playcontent/1-s2.0-S000293431300870X.

[48] W.M. Smith, F. Riddell, M. Madon BSc, M.J. Gleva, Comparison of diagnostic value using a small, single channel, P-wave centric sternal ECG monitoring patch with a standard 3-lead Holter system over 24 hours, American Heart Journal, Vol. 185, Iss. March, 2016, pp. 67-73. https://www.clinicalkey.es/playcontent/1-s2.0-S0002870316302733.

[49] Operator's Manual NorthEast Monitoring, Inc. DR180+ Digital Recorder, web page. Available (accessed webpage 15/05): http://nemon.com/supportfiles/NEMM001-Rev-K_DR180+_Manual.pdf.

[50] Ambu Ambu® BlueSensor P
, web page. Available (accessed 07/05): https://www.ambu.com/products/cardiology/ecg-electrodes/product/ambu-bluesensor-p.

[51] A. Ambu Ambu® BlueSensor N, web page. Available (accessed 07/05): https://www.ambu.com/products/cardiology/ecg-electrodes/product/ambu-bluesensor-n.

[52] Metting van Rijn, A C, A. Peper, C.A. Grimbergen, High-quality recording of bioelectric events. Part 1. Interference reduction, theory and practice, Medical & biological engineering & computing, Vol. 28, Iss. 5, 1990, pp. 389-397. http://www.ncbi.nlm.nih.gov/pubmed/2277538.

[53] S. Nishimura, Y. Tomita, T. Horiuchi, Clinical application of an active electrode using an operational amplifier, IEEE Transactions on Biomedical Engineering, Vol. 39, Iss. 10, 1992, pp. 1096-1099. https://ieeexplore.ieee.org/document/161342.

[54] Texas Instruments High-Precision, Low-Noise, Rail-to-Rail Output, 11-MHz JFET Op Amp, web page. Available (accessed 15/04): http://www.ti.com/lit/ds/symlink/ads1299.pdf.

[55] Andrews Ryan Three guidelines for designing anti-aliasing filters, web page. Available (accessed 09/05): https://e2e.ti.com/blogs_/archives/b/precisionhub/archive/2015/11/06/three-guidelines-for-designing-anti-aliasing-filters.

[56] Texas Instruments EEG Front-End Performance Demonstration Kit, web page. Available (accessed 09/05): http://www.ti.com/lit/ug/slau443b/slau443b.pdf.

[57] Texas Instruments ADS1299-x Low-Noise, 4-, 6-, 8-Channel, 24-Bit, Analog-to-Digital Converter for EEG and
Biopotential Measurements, Texas Instruments, web page. Available (accessed 04/04): http://www.ti.com/lit/ds/symlink/ads1299.pdf.

[58] B.J. Drew, R.M. Califf, M. Funk, E.S. Kaufman, M.W. Krucoff, M.M. Laks, P.W. Macfarlane, C. Sommargren, S. Swiryn, G.F. Van Hare, Practice Standards for Electrocardiographic Monitoring in Hospital Settings: An American Heart Association Scientific Statement From the Councils on Cardiovascular Nursing, Clinical Cardiology, and Cardiovascular Disease in the Young: Endorsed by the International Society of Computerized Electrocardiology and the American Association of Critical-Care Nurses, Circulation, Vol. 110, Iss. 17, 2004, pp. 2721-2746. http://circ.ahajournals.org/cgi/content/abstract/110/17/2721.

[59] I. BIOPAC Systems BIONOMADIX SERIES Productsheet
, web page. Available (accessed 04/04): https://www.biopac.com/wp-content/uploads/BioNomadix-Series.pdf.

[60] M. Puurtinen, J. Viik, J. Hyttinen, Best Electrode Locations for a Small Bipolar ECG Device: Signal Strength Analysis of Clinical Data, Annals of Biomedical Engineering, Vol. 37, Iss. 2, 2009, pp. 331-336. http://www.ncbi.nlm.nih.gov/pubmed/19020977.

[61] I.H. Hansen, K. Hoppe, A. Gjerde, J.K. Kanters, H.B.D. Sorensen, Comparing twelve-lead electrocardiography with close-to-heart patch based electrocardiography, 2015 37th Annual International Conference of the IEEE Engineering in Medicine and Biology Society (EMBC), Milan, Italy, IEEE, United States, pp. 330-333.

[62] R. Fensli, T. Gundersen, T. Snaprud, O. Hejlesen, Clinical evaluation of a wireless ECG sensor system for arrhythmia diagnostic purposes, Medical Engineering and Physics, Vol. 35, Iss. 6, 2013, pp. 697-703. https://www.clinicalkey.es/playcontent/1-s2.0-S1350453313000556.

[63] F. Kornreich, Clinical Utility of Body Surface Potential Mapping, Cardiac Electrophysiology Review, Vol. 1, Iss. 3, 1997, pp. 304.

[64] F. Buendía-Fuentes, M.A. Arnau-Vives, A. Arnau-Vives, Y. Jiménez-Jiménez, J. Rueda-Soriano, E. Zorio-Grima, A. Osa-Sáez, L.V. Martínez-Dolz, L. Almenar-Bonet, M.A. Palencia-Pérez, High-Bandpass Filters in Electrocardiography: Source of Error in the Interpretation of the ST Segment, ISRN Cardiology, Vol. 2012, Iss. June, 2012, pp. 1-10.

APPENDIX A: ACTIVE ELECTRODE PCB LAYOUT (TOP & BOTTOM LAYER)